ORIGINAL RESEARCH

Metabolomics Profiling of Visceral Adipose Tissue: Results From MESA and the NEO Study

Ian J. Neeland, MD; Sebastiaan C. Boone, PhD; Dennis O. Mook-Kanamori, MD, PhD; Colby Ayers, MS; Roelof A. J. Smit, PhD; Ioanna Tzoulaki, PhD; Ibrahim Karaman, PhD; Claire Boulange, PhD; Dhananjay Vaidya, MBBS, MPH, PhD; Naresh Punjabi, MD, PhD; Matthew Allison, MD, MPH; David M. Herrington, MD; J. Wouter Jukema, PhD; Frits R. Rosendaal, PhD; Hildo J. Lamb, PhD; Ko Willems van Dijk, PhD; Philip Greenland, MD; Renée de Mutsert, PhD

***Background*—**Identifying associations between serum metabolites and visceral adipose tissue (VAT) could provide novel biomarkers of VAT and insights into the pathogenesis of obesity-related diseases. We aimed to discover and replicate metabolites reflecting pathways related to VAT.

***Methods and Results*—**Associations between fasting serum metabolites and VAT area (by computed tomography or magnetic resonance imaging) were assessed with cross-sectional linear regression of individual-level data from participants in MESA (Multi-Ethnic Study of Atherosclerosis; discovery, N=1103) and the NEO (Netherlands Epidemiology of Obesity) study (replication, N=2537). Untargeted ^{1}H nuclear magnetic resonance metabolomics profiling of serum was performed in MESA, and metabolites were replicated in the NEO study using targeted ^{1}H nuclear magnetic resonance spectroscopy. A total of 30 590 metabolomic spectral variables were evaluated. After adjustment for age, sex, race/ethnicity, socioeconomic status, smoking, physical activity, glucose/lipid-lowering medication, and body mass index, 2104 variables representing 24 nonlipid and 49 lipid/lipoprotein subclass metabolites remained significantly associated with VAT (P=4.88×10^{-20}–1.16×10^{-3}). These included conventional metabolites, amino acids, acetylglycoproteins, intermediates of glucose and hepatic metabolism, organic acids, and subclasses of apolipoproteins, cholesterol, phospholipids, and triglycerides. Metabolites mapped to 31 biochemical pathways, including amino acid substrate use/metabolism and glycolysis/gluconeogenesis. In the replication cohort, acetylglycoproteins, branched-chain amino acids, lactate, glutamine (inversely), and atherogenic lipids remained associated with VAT (P=1.90×10^{-35}–8.46×10^{-7}), with most associations remaining after additional adjustment for surrogates of VAT (glucose level, waist circumference, and serum triglycerides), reflecting novel independent associations.

***Conclusions*—**We identified and replicated a metabolite panel associated with VAT in 2 community-based cohorts. These findings persisted after adjustment for body mass index and appear to define a metabolic signature of visceral adiposity. **(*J Am Heart Assoc*. 2019;8:e010810. DOI: 10.1161/JAHA.118.010810.)**

Key Words: adipose tissue • cohort • metabolite • metabolomics • obesity • visceral adipose tissue

Although obesity is associated with increased risk of diabetes mellitus and cardiovascular disease (CVD), many obese individuals remain free of cardiometabolic disease.[1] One factor that contributes to the heterogeneity of risk among obese individuals is the amount of visceral adipose tissue (VAT).[2] Excess VAT is associated with insulin resistance, atherogenic dyslipidemia, and hepatic steatosis[3]; and in the long-term, excess VAT has been linked with

From the Division of Cardiology, Departments of Internal Medicine (I.J.N.) and Clinical Sciences (C.A.), University of Texas Southwestern Medical Center, Dallas, TX; Departments of Clinical Epidemiology (S.C.B., D.O.M.-K., R.A.J.S., F.R.R., R.d.M.), Public Health and Primary Care (D.O.M.-K.), Cardiology (J.W.J.), Radiology (H.J.L.), Human Genetics (K.W.v.D.), and Internal Medicine (K.W.v.D.), Einthoven Laboratory for Experimental Vascular Medicine (K.W.v.D.), Leiden University Medical Center, Leiden, the Netherlands; Department of Epidemiology and Biostatistics (I.T., I.K.) and Metabometrix Ltd (C.B.), Imperial College London, London, United Kingdom; Department of Medicine, Johns Hopkins University, Baltimore, MD (D.V., N.P.); Department of Family Medicine and Public Health, University of California San Diego, La Jolla, CA (M.A.); Department of Medicine, Wake Forest University, Winston Salem, NC (D.M.H.); and Department of Preventive Medicine, Northwestern University, Chicago, IL (P.G.).

Accompanying Data S1, Tables S1 through S3 and Figures S1, S2 are available at https://www.ahajournals.org/doi/suppl/10.1161/JAHA.118.010810

Correspondence to: Ian J. Neeland, MD, University of Texas Southwestern Medical Center, 5323 Harry Hines Blvd, Dallas TX, 75390-8830. E-mail: ian.neeland@utsouthwestern.edu

Received November 9, 2018; accepted February 19, 2019.

Clinical Perspective

What Is New?

- We identified and validated a metabolite signature associated with visceral adipose tissue from a single fasting blood sample in 2 large epidemiological cohort studies.

What Are the Clinical Implications?

- These findings provide insight into potential mechanisms underpinning visceral adipose tissue metabolism distinct from generalized obesity defined by the body mass index.
- Blood-based metabolic profiling of visceral adipose tissue using a limited set of important metabolites may address the implementation gap between recognizing the role of visceral adiposity in cardiometabolic disease and actually assessing it clinically.

increases in the risk of developing type 2 diabetes mellitus[4] and the metabolic syndrome,[5] across the spectrum of body mass index (BMI).

Currently, precise measures of VAT are only obtainable through assessment with advanced imaging techniques, such as computed tomography and magnetic resonance imaging (MRI). Determination of VAT burden and its application to prevention or treatment of cardiometabolic outcomes are, therefore, not currently practical for routine clinical use. Anthropometric approximations, like waist circumference, are not sufficient to assess risk associated with VAT,[6] and specific blood-based metabolic markers reflecting pathways related to VAT are lacking.

The development of high-throughput metabolomics profiling has made it feasible to acquire profiles of a whole organism's metabolic status.[7] The metabolome profile can provide a high-resolution and reproducible phenotypic signature of complex disease states, such as type 2 diabetes mellitus,[8] and may offer useful biologic information that can help with understanding molecular pathways in disease. At present, there are limited data on the relationship between metabolite profiles and variation in body fat distribution, especially with VAT. Studies to date have been composed of relatively small sample sizes,[9,10] a finite number of targeted metabolites,[11] or histological samples of adipose tissue alone.[12] Targeting blood-based metabolites from sufficiently large numbers of people may yield more robust and reproducible results from samples that are more easily obtained in clinical practice. Therefore, we aimed to use data from 2 large independent cohorts, MESA (Multi-Ethnic Study of Atherosclerosis) and the NEO (Netherlands Epidemiology of Obesity) study, to discover and replicate metabolites reflecting various pathways related to visceral fat; and we performed a mendelian randomization analysis to explore the potential causal effects of atherogenic dyslipidemia on VAT deposition.

Methods

The data that support the findings of this study are available from the corresponding author on reasonable request.

Study Population and Variable Definitions

Multi-Ethnic Study of Atherosclerosis

The overall design of MESA has been described previously.[13] Briefly, MESA consists of 6814 men and women, aged 45 to 84 years, who were free of clinical CVD, of different ethnicities (white, black, Chinese American, and Hispanic) and enrolled from 6 different sites in the United States. Clinical CVD was defined as history of myocardial infarction, angina pectoris, prior revascularization, heart failure, atrial fibrillation, stroke, or peripheral arterial disease at the time of enrollment. Baseline medical history, anthropometric measurements, and laboratory data for the present study were taken from the first examination of MESA cohort (July 2000 to August 2002), as previously described.[14] Education level and yearly income were determined from a self-reported questionnaire. Physical activity was derived using a self-reported frequency and type of leisure time physical activity and a standard conversion for metabolic equivalence units.[15] Fasting serum samples from 3955 participants randomly selected were collected at the baseline visit to generate untargeted metabolomics profiles in a subset of MESA participants as part of the Development of Combinatorial Biomarkers for Subclinical Atherosclerosis initiative, a collaboration between MESA investigators and scientists at Imperial College London, as described below. At examinations 2 or 3, a random subset of 1970 MESA participants underwent abdominal computed tomography scans for aortic calcium that were subsequently used for quantifying visceral fat area: visit 2, n=756; visit 3, n=1172. For the purposes of the current study, we included 1103 participants with completed assessments of metabolomics and visceral fat. The median (interquartile range) time between metabolomics and VAT assessments was 3.2 (3.0–3.4) years.

The NEO study

The NEO study is a population-based, prospective cohort study, including 6671 individuals aged 45 to 65 years, with an oversampling of individuals with overweight or obesity.[16] Between September 2008 and 2012, men and women living in the greater area of Leiden (in the West of the Netherlands) were invited to participate if they were aged between 45 and 65 years and had a self-reported BMI of $\geq$27 kg/m^2. In

addition, all inhabitants, aged between 45 and 65 years, from one municipality (Leiderdorp) were invited to participate, irrespective of their BMI, allowing for a reference distribution of BMI. To correctly represent associations in the Dutch general population, adjustments for this oversampling have been made in the analyses[17] by weighting individuals toward the BMI distribution of participants from the Leiderdorp municipality, whose BMI distribution was similar to the BMI distribution of the general Dutch population. Consequently, the results of the analyses in the NEO study apply to a population-based study without oversampling of individuals with a BMI $\geq$27 kg/m^2.

Participants were invited to a baseline visit at the NEO study center after an overnight fast. Before this study visit, participants completed a general questionnaire at home to report demographic, lifestyle, and clinical information. At the baseline visit, an extensive physical examination was performed, including blood sampling. A high-throughput proton nuclear magnetic resonance (NMR) metabolomics platform (Nightingale Health Ltd, Helsinki, Finland) was used to quantify 224 lipid and metabolite measures in all participants, as described below. VAT area was quantified using MRI in 2580 participants who were randomly selected from those without contraindications for MRI. After exclusion of missing data (failed MRI, n=11; failed blood sampling, n=33), 2536 participants were analyzed. Of these participants, analysis or annotation of separate metabolites failed in a median of 0.26% (interquartile range, 0.03%–3.49%), which were not imputed in the statistical analyses. Protocols were approved by the Institutional Review Board at each participating institution for MESA and by the Medical Ethical Committee of the Leiden University Medical Center for the NEO study. All participants provided written informed consent.

Metabolomics Measurements

In MESA (the discovery cohort), untargeted ^{1}H NMR analysis of serum samples obtained at the baseline examination was performed using a method previously described.[18] MESA samples used in the current study were analyzed in 2 phases as part of the European Union–funded Development of Combinatorial Biomarkers for Subclinical Atherosclerosis project. Details about the preparation of samples, including quality controls, NMR data acquisition, and NMR data processing, are described in Data S1. The specific NMR data sets used in the current study include the following: (1) standard 1-dimensional NMR spectrum showing resonances from all proton-containing molecules in the sample, including broad, largely undefined bands from serum proteins, sharper and well-defined bands from serum lipoproteins (with some classification into their main groups), and sharp peaks from a range of small-molecule metabolites, such as amino acids, simple carbohydrates, organic acids, organic bases, and several osmolytes; (2) Carr-Purcell-Meiboom-Gill spectrum that attenuates the peaks from the macromolecules and allows better definition of the small molecules; and (3) quantification of lipoprotein subclasses obtained from deconvolution of the methyl peak near δ0.89 using a Bruker (Bruker Biospin, Rheinstetten, Germany) procedure adapted from the method of Petersen et al.[19] Bruker NMR measurements included total high-density lipoprotein (HDL), low-density lipoprotein (LDL), triglycerides, and cholesterol as well as analysis of 105 lipoprotein subclasses, including different chemical components of intermediate-density lipoprotein (density, 1.006–1.019 kg/L), very-LDL (VLDL; density, 0.950–1.006 kg/L), LDL (density, 1.09–1.63 kg/L), and HDL (density, 1.063–1.210 kg/L). The LDL subfraction was separated into 6 density classes (LDL-1, 1.019–1.031 kg/L; LDL-2, 1.031–1.034 kg/L; LDL-3, 1.034–1.037 kg/L; LDL-4, 1.037–1.040 kg/L; LDL-5, 1.040–1.044 kg/L; and LDL-6, 1.044–1.063 kg/L), and the HDL subfraction was separated into 4 density classes (HDL-1, 1.063–1.100 kg/L; HDL-2, 1.100–1.125 kg/L; HDL-3, 1.125–1.175 kg/L; and HDL-4, 1.175–1.210 kg/L). These specific NMR spectra have been previously tested for quality control, harmonization, and alignment.[20]

In the NEO study (the replication cohort), targeted metabolomics were measured using a high-throughput proton NMR metabolomics platform (Nightingale Health Ltd) to quantify 224 lipid and metabolite measures in all participants. The NMR spectroscopy was conducted at the Medical Research Council Integrative Epidemiology Unit at the University of Bristol (Bristol, UK) and processed by Nightingale's biomarker quantification algorithms (version 2014). This method provides quantification of lipoprotein subclass profiling with lipid concentrations within 14 lipoprotein subclasses. The 14 subclass sizes were defined as follows: extremely large VLDL with particle diameters from 75 nm upwards and a possible contribution of chylomicrons, 5 VLDL subclasses (average particle diameters, 64.0, 53.6, 44.5, 36.8, and 31.3 nm), intermediate-density lipoprotein (average particle diameter, 28.6 nm), 3 LDL subclasses (average particle diameters, 25.5, 23.0, and 18.7 nm), and 4 HDL subclasses (average particle diameters, 14.3, 12.1, 10.9, and 8.7 nm). Within the lipoprotein subclasses, the following components were quantified: total cholesterol, total lipids, phospholipids, free cholesterol, cholesteryl esters, and triglycerides. The mean size for VLDL, LDL, and HDL particles was calculated by weighting the corresponding subclass diameters with their particle concentrations. Furthermore, 58 metabolic measures were determined that belong to classes of apolipoproteins, cholesterol, fatty acids, glycerides, phospholipids, amino acids, fluid balance, glycolysis-related

metabolites, inflammation, and ketone bodies. Details of the experimentation and applications of the NMR metabolomics platform have been described previously,[21] as well as CVs (coefficients of variation) for metabolic biomarkers.[22,23] A full list of the measured biomarkers in the NEO study is included in Table S1.

Body Fat and VAT Measurements

In MESA, weight and height were measured using a balance-beam scale and stadiometer, respectively, and used to calculate BMI as weight (in kilograms) divided by height (in meters) squared. Waist circumference was measured at the minimum abdominal girth using a steel measuring tape of standard 4-ounce tension in centimeters. Electron-beam or multidetector computed tomography scans of the abdomen, obtained to measure aortic calcification, were used to measure fat and lean area in the abdomen, as previously described.[5] Briefly, visceral fat was defined as the fat enclosed by the visceral cavity, and fat tissue was identified as being between −190 and −30 Hounsfield units. Within the area of interest, the density value was assigned to each pixel using the MIPAV 4.1.2 software (National Institutes of Health, Bethesda, MD) as fat or lean tissue. Six transverse cross-sectional slices were analyzed (2 at L2–3, 2 at L3–4, and 2 at L4–5), and visceral fat area (cm^2) was calculated as the average of the sum of visceral fat over all 6 available slices. Interreader and intrareader reliability for visceral fat area was 0.99 for all measures.

In the NEO study, body weight was assessed by the Tanita bioimpedance balance (TBF-310; Tanita International Division, UK) without shoes, and 1 kg was subtracted from the body weight. Waist circumference was measured midway between the border of the lower costal margin and the iliac crest. Abdominal visceral fat was quantified by a turbo spin echo imaging protocol using MRI. Imaging was performed on a 1.5-T MR system (Philips Medical Systems, Best, the Netherlands). At the level of the fifth lumbar vertebra, 3 transverse images, each with a slice thickness of 10 mm, were obtained during a breath hold. Visceral fat area was quantified by converting the number of pixels to square centimeters for all 3 slides, and the mean area of the 3 slides was used in the analyses. Earlier studies have shown that such cross-sectional images are highly correlated to total volumes (correlation coefficients, ≈0.8) and can, therefore, validly represent VAT.[24]

Statistical Analysis

Baseline characteristics of the study populations are presented as median (interquartile range) or proportion (percentage), as appropriate. Multivariable linear regression models were constructed to assess the association of metabolites with VAT for all NMR experiments. To allow for comparisons, metabolites were logarithmically transformed and standardized to a mean of 0 and an SD of 1. VAT was confirmed to be normally distributed. Linear regression modeling was performed, with the metabolite as the exposure variable and mean VAT area as the outcome variable, on the basis of a hypothesis-free design because the biological features of metabolomics and VAT may be bidirectional (ie, metabolites may influence VAT accumulation/function, and/or VAT accumulation may influence downstream metabolic processes). Furthermore, to uncover potential causal pathways to visceral fat accumulation, we also performed mendelian randomization analyses with the replicated metabolites, where possible (see method below). Models were adjusted for age, sex, race/ethnicity, socioeconomic status, smoking, physical activity, glucose and lipid-lowering medication use, and BMI to investigate to what extent the associations were specific for VAT and not merely overall body mass. Given the hypothesis-free design and the large number of comparisons, we adjusted for multiple testing using a predefined false-discovery rate threshold of 1% for the primary analysis. Given known differences in body fat distribution by sex and race/ethnicity, secondary analyses were performed, stratified by these variables. We also performed targeted pathway analysis using Metaboanalyst (http://www.metaboanalyst.ca), a web-based tool for metabolomics analysis, and interpretation that uses the Kyoto Encyclopedia of Genes and Genomes and Small Molecule Pathway databases to perform overrepresentation, pathway enrichment, and pathway topological analyses (explained in Data S1). They were used to determine the overall associations of our metabolite set that map to particular pathways related to VAT and assess whether the metabolites are critical connectors within the pathways' network structure.[25]

Next, we used the NEO study as a separate cohort to replicate our findings with the same statistical analysis strategy on a targeted metabolomics platform. All analyses in the NEO study were weighted toward the BMI distribution of the general population. A predefined false-discovery rate threshold of 1% was also used for this analysis. Using the replicated metabolites, to identify novel VAT-associated metabolites beyond known correlates, we additionally sequentially adjusted for the following: (1) fasting glucose concentrations and waist circumference; and (2) plasma triglyceride concentrations, to investigate if and what metabolites remained after adjustment for additional modifiers of metabolic disease and indirect surrogate markers for VAT (eg, "hypertriglyceridemic waist").[26] Finally, to better understand the potential directionality of the association between lipid-based metabolites and VAT (ie, does dyslipidemia influence VAT deposition), we estimated the potential causal effects of overall measures of HDL cholesterol (HDL-C), LDL cholesterol,

and triglycerides on VAT volume by performing 2-sample mendelian randomization analyses using genetic instruments linked to blood lipid levels and combining the summary statistics of large genome-wide meta-analyses on blood lipid levels and VAT (explained in Data S1). Statistical analyses were performed using SAS software, version 9.4 (SAS Corporation, Cary, NC), and Stata Statistical Software, version 14.0 (Statacorp, College Station, TX).

Results

Characteristics of the discovery and replication study cohorts are presented in Table 1. Both cohorts were primarily middle aged, with ≈50% women. MESA cohort was racially/ethnically diverse, with ≈60% nonwhite participants, compared with the NEO study cohort, which was predominantly white. The median BMIs, waist circumferences, and VAT areas for women and men were modestly higher in MESA than in the NEO study, generally reflecting known demographic and anthropometric differences between the United States and the Netherlands.

Metabolite Profiling in MESA

In MESA discovery cohort, 30 590 metabolomic spectral variables were evaluated in untargeted metabolomics analyses using NMR. After multivariable adjustment for age, sex, race/ethnicity, socioeconomic status, smoking, physical activity, glucose and lipid-lowering medication use, and BMI, 2104 spectral variables representing 24 nonlipid (Table 2) and 49 lipid/lipoprotein subclass metabolites (Table 3) remained statistically significantly associated with VAT ($P=4.88\times10^{-20}$–1.16×10^{-3}). These included conventional clinical metabolites (eg, creatinine), amino acids and their byproducts (eg, leucine, isoleucine, glutamine [inversely associated], valine, and proline), acetylglycoproteins and mannose, intermediates of glucose and hepatic metabolism (eg, glycerol, glucose, and choline), organic acids (eg, lactate), subclasses of very-low-density, low-density, intermediate-density, and high-density apolipoproteins, cholesterol, phospholipids, and triglycerides. In general, among the lipid-based metabolites, HDL-related metabolites were inversely associated with VAT. Conversely, intermediate-density lipoprotein and VLDL particles were almost uniformly positively associated with VAT. Metabolite profiles were generally consistent between men and women and between white and nonwhite participants in stratified analyses (Figures S1 and S2).

Pathway analyses were performed using overrepresentation, pathway enrichment, and pathway topological analysis methods for the nonlipid metabolites. Thirty-one distinct biochemical pathways were identified, mapping to the metabolite set significantly associated with VAT (Figure 1). The pathways with the strongest associations with visceral adiposity (based on *P* values derived from pathway enrichment analyses reflecting the overall association of the metabolite set) included those using amino acids as substrates for biosynthetic processes, such as aminoacyl-tRNA biosynthesis ($P=3.39\times10^{-10}$) and branched-chain amino acid degradation ($P=1.30\times10^{-4}$). Other pathways included metabolism of other amino acids and glycolysis/gluconeogenesis. A full list of the metabolic pathways associated with visceral adiposity and centrality/impact of the metabolites on each specific pathway is given in Table S2.

Replication Analysis: The NEO Study

To replicate our findings from MESA in a different epidemiological cohort, we repeated the analyses with the metabolites that were significantly associated with VAT in the discovery cohort by using the targeted Nightingale metabolomics platform in the NEO study cohort. In this analysis, 6 of the nonlipid (Table 2) and 34 of the lipid/lipoprotein subclass metabolites (Table 3) were replicated and retained statistical significance in the NEO study using a prespecified false-discovery rate 1% threshold. The β coefficients (reflecting the magnitude of association between metabolites and VAT) were highly correlated between MESA and the NEO study ($R^2=0.68$, Figure 2). Unadjusted correlations between adiposity variables and replicated metabolites in both MESA and the NEO study are reported in Table S3. Similar patterns for metabolite-VAT associations in sex- and race/ethnicity-stratified analyses were seen in the replication cohort as in the discovery cohort (Figures S1 and S2).

Among the replicated metabolites (selecting HDL-C, VLDL cholesterol, and serum triglycerides to represent the broad categories of related lipids/lipoproteins associated with VAT), we performed sequential adjustment for fasting glucose concentrations and waist circumference and found the associations between the selected replicated metabolites and VAT were slightly weaker but retained statistical significance (Figure 3). After further adjustment for plasma triglyceride concentrations (accounting for hypertriglyceridemic waist), acetylglycoproteins, branched-chain amino acids (isoleucine, leucine, and valine), glutamine (inversely), and serum triglycerides remained significantly associated with VAT (nominal $P<0.05$ for all, Figure 3).

Mendelian Randomization Study

Two-sample mendelian randomization analyses using genetic instruments for blood lipid levels were performed by combining the summary statistics of large-scale genome-wide

Table 1. Baseline Characteristics of the Study Populations

Clinical Characteristics	MESA (n=1103)	NEO Study (n=2536)
Demographics		
Age, y	63.0 (54.0–70.0)	56.0 (51.0–61.0)
Men, %	51.6	47.5
Race/ethnicity, %		
White	39.8	95.9
Black	17.6	. . .
Hispanic	27.9	. . .
Chinese	14.7	. . .
Other	. . .	4.1
Education level, %		
Low (some or graduated high school)	35.5	53.7
High (vocational school, university, and postgraduate)	64.5	46.3
Income, $/y, %		
0–34 999	43.9	N/A
35 000–99 999	39.8	N/A
≥100 000	16.4	N/A
Medical history		
Hypertension, %	48.5	19.7
Diabetes mellitus, %	11.4	3.3
Dyslipidemia, %	43.9	42.5
Metabolic syndrome, %	34.5	23.7
Current smoker, %	14.1	14.4
Moderate and vigorous physical activity, MET×min/wk	4001.3 (2032.5–7260.0)	2850.0 (1597.5–4905.0)
Systolic BP, mm Hg	124.0 (111.0–141.0)	129.0 (118.0–141.0)
Diastolic BP, mm Hg	72.0 (65.0–79.0)	83.0 (76.0–90.0)
BP ≥130/85 mm Hg, %	36.0	56.0
Triglycerides, mg/dL	119.0 (79.0–175.0)	90.3 (64.6–131.9)
Triglycerides ≥150 mg/dL, %	35.1	19.0
HDL-C, mg/dL	48.0 (40.0–59.0)	57.9 (47.5–71.4)
HDL-C <40 mg/dL (men) or <50 mg/dL (women), %	35.8	15.4
Fasting glucose, mg/dL	91.0 (84.0–99.0)	95.3 (89.7–102.5)
Fasting glucose ≥100 mg/dL, %	24.9	32.3
Body composition		
BMI, kg/m^2	Women: 27.3 (24.4–31.3)	Women: 24.9 (22.0–27.5)
	Men: 27.2 (24.4–30.1)	Men: 26.3 (24.2–28.5)
Waist circumference, cm	Women: 96.0 (85.8–105.1)	Women: 84.0 (77.0–94.0)
	Men: 97.5 (90.6–106.3)	Men: 97.0 (91.0–104.0)
Waist circumference ≥102 cm (men) or ≥88 cm (women), %	Women: 70.0	Women: 38.0
	Men: 36.4	Men: 32.6
VAT area, cm^2	Women: 122.4 (82.1–183.0)	Women: 56.8 (36.6–89.0)
	Men: 191.6 (128.0–248.3)	Men: 105.6 (75.1–144.2)

Data are presented as median (interquartile range) or proportion (percentage), as appropriate. Results from the NEO study are based on analyses weighted toward the BMI distribution of the general population. Number of missing values per variable in the NEO study: ethnicity, 4; education, 26; hypertension, 6; diabetes mellitus, 7; metabolic syndrome, 7; smoking, 3; physical activity, 11; diastolic BP, 1; triglycerides, 6; HDL-C, 6; and fasting glucose, 9 (no missing values for other variables). BMI indicates body mass index; BP, blood pressure; HDL-C, high-density lipoprotein cholesterol; MESA, Multi-Ethnic Study of Atherosclerosis; MET, metabolic equivalent; N/A, not applicable; NEO, Netherlands Epidemiology in Obesity; VAT, visceral adipose tissue.

Table 2. Associations Between Nonlipid Metabolites and VAT

MESA			NEO Study		
Metabolite	Effect Estimate β (95% CI)	Nominal *P* Value	Metabolite	Effect Estimate β (95% CI)	Nominal *P* Value
1-Dimensional NMR					
Acetylglycoproteins	14.50 (10.87 to 18.13)	1.14E-14	Acetylglycoproteins	11.70 (9.86 to 13.54)	1.58E-34*
Choline	−15.54 (−19.42 to −11.66)	9.52E-15	…	…	…
Creatinine	12.88 (9.30 to 16.45)	2.97E-12	Creatinine	1.21 (−0.75 to 3.16)	2.25E-01
Glycerol	8.43 (4.65 to 12.20)	1.33E-05	…	…	…
Glyceryl groups of lipids	13.83 (10.29 to 17.36)	4.15E-14	…	…	…
Lactate	13.73 (10.14 to 17.32)	1.38E-13	Lactate	4.75 (2.86 to 6.63)	8.46E-07*
Mannose	15.92 (12.33 to 19.52)	1.49E-17	…	…	…
Myoinositol	7.96 (4.24 to 11.69)	3.05E-05	…	…	…
Proline	12.90 (9.21 to 16.59)	1.26E-11	…	…	…
Carr-Purcell-Meiboom-Gill echo acquisition					
2-Ketoisovalerate	3.35 (2.24 to 4.46)	4.73E-09	…	…	…
Acetylglycoproteins	9.22 (6.81 to 11.63)	1.41E-13	Acetylglycoproteins	11.70 (9.86 to 13.54)	1.58E-34*
Alanine	−3.50 (−4.68 to −2.33)	5.98E-09	…	…	…
Albumin	−1.88 (−2.40 to −1.35)	5.98E-12	Albumin	−0.02 (−1.80 to 1.76)	9.84E-01
α-Glucose	−8.34 (−11.40 to −5.27)	1.19E-07	…	…	…
Arginine	1.01 (0.59 to 1.43)	3.25E-06	…	…	…
β-Glucose	−3.29 (−4.47 to −2.11)	5.99E-08	…	…	…
Choline	−6.45 (−8.56 to −4.34)	3.00E-09	…	…	…
Citrate	−0.30 (−0.47 to −0.14)	2.79E-04	…	…	…
Creatinine	2.99 (2.19 to 3.78)	3.74E-13	Creatinine	1.21 (−0.75 to 3.16)	2.25E-01
Ornithine	−1.62 (−2.41 to −0.84)	5.64E-05	…	…	…
Glutamate	0.33 (0.14 to 0.51)	5.04E-04	…	…	…
Glutamine	−1.63 (−2.24 to −1.03)	1.42E-07	Glutamine	−3.09 (−5.05 to −1.13)	2.01E-03*
Glyceryl groups of lipids	2.02 (1.54 to 2.50)	4.18E-16	…	…	…
Isoleucine	2.50 (1.88 to 3.12)	5.25E-15	Isoleucine	13.22 (11.16 to 15.28)	3.78E-35*
Lactate	6.44 (4.81 to 8.07)	2.44E-14	Lactate	4.75 (2.86 to 6.63)	8.46E-07*
Leucine	3.65 (2.50 to 4.79)	7.03E-10	Leucine	12.58 (10.36 to 14.80)	5.23E-28*
Lysine	−8.96 (−10.94 to −6.98)	3.25E-18	…	…	…
Mannose	11.42 (9.02 to 13.81)	4.88E-20	…	…	…
Proline	5.54 (4.12 to 6.96)	5.47E-14	…	…	…
Pyroglutamate	−1.05 (−1.36 to −0.73)	1.15E-10	…	…	…
Valine	3.05 (1.95 to 4.15)	6.55E-08	Valine	6.89 (4.68 to 9.10)	1.07E-09*

Model adjusted for age, sex, race/ethnicity, socioeconomic status, smoking, physical activity, glucose and lipid-lowering medication use, and body mass index. Effect estimate β represents the difference in VAT area (in cm^2) per 1-SD in metabolite intensity (relative units). MESA indicates Multi-Ethnic Study of Atherosclerosis; NEO, Netherlands Epidemiology in Obesity; NMR, nuclear magnetic resonance; VAT, visceral adipose tissue.
*Metabolites that were significant in the NEO study data set after false-discovery rate correction.

meta-analyses on blood lipid levels and VAT. Data on both the instrument-exposure (blood lipid levels) and instrument-outcome (VAT volume) associations were available for 208 instruments (HDL-C, n=83; LDL cholesterol, n=72; triglycerides, n=53; with 9 serving as instruments for multiple traits), after harmonization. As shown in Figure S3, we did not find evidence for a causal effect of overall measures of HDL-C, LDL cholesterol, and triglyceride blood levels on VAT volume

Table 3. Associations Between Lipid Metabolites and VAT

MESA			NEO Study		
Metabolite	Effect Estimate β (95% CI)	Nominal *P* Value	Metabolite	Effect Estimate β (95% CI)	Nominal *P* Value
HDL cholesterol	−11.00 (−14.74 to −7.25)	1.14E-08	HDL cholesterol	−8.11 (−10.21 to −6.00)	5.67E-14*
HDL free cholesterol	−13.21 (−17.15 to −9.27)	7.81E-11	…	…	…
HDL phospholipids	−11.50 (−15.50 to −7.50)	2.22E-08	…	…	…
Total plasma apolipoprotein-A1	−7.59 (−11.36 to −3.81)	8.84E-05	Total plasma apolipoprotein-A1	−2.94 (−5.04 to −0.84)	6.09E-03*
Extralarge HDL apolipoprotein-A1	−10.92 (−14.75 to −7.10)	2.82E-08	…	…	…
Extralarge HDL cholesterol	−10.72 (−14.56 to −6.89)	5.47E-08	Extralarge HDL cholesterol	−7.52 (−9.61 to −5.44)	1.99E-12*
Extralarge HDL free cholesterol	−12.88 (−16.61 to −9.15)	2.18E-11	Extralarge HDL free cholesterol	−8.24 (−10.34 to −6.13)	2.49E-14*
Extralarge HDL phospholipids	−12.78 (−16.92 to −8.63)	2.12E-09	Extralarge HDL phospholipids	−10.66 (−12.83 to −8.49)	1.65E-21*
Large HDL apolipoprotein-A1	−8.90 (−13.38 to −4.41)	1.07E-04	…	…	…
Large HDL cholesterol	−10.68 (−14.48 to −6.89)	4.33E-08	Large HDL cholesterol	−10.99 (−13.07 to −8.92)	8.21E-25*
Large HDL free cholesterol	−12.72 (−16.66 to −8.78)	3.76E-10	Large HDL free cholesterol	−10.98 (−13.00 to −8.95)	9.22E-26*
Large HDL phospholipids	−10.90 (−14.80 to −6.99)	5.66E-08	Large HDL phospholipids	−9.52 (−11.67 to −7.37)	7.09E-18*
Medium HDL cholesterol	−9.15 (−12.95 to −5.35)	2.70E-06	Medium HDL cholesterol	−3.58 (−5.63 to −1.54)	5.92E-04*
Medium HDL free cholesterol	−9.83 (−14.01 to −5.65)	4.56E-06	Medium HDL free cholesterol	−3.52 (−5.61 to −1.44)	9.37E-04*
Medium HDL phospholipids	−7.88 (−11.78 to −3.97)	8.33E-05	Medium HDL phospholipids	−1.61 (−3.68 to 0.46)	1.27E-01
Medium HDL triglycerides	6.44 (2.56 to 10.31)	1.16E-03	Medium HDL triglycerides	8.65 (6.37 to 10.92)	1.26E-13*
Small HDL triglycerides	11.31 (7.78 to 14.84)	4.87E-10	Small HDL triglycerides	10.65 (8.91 to 12.39)	2.31E-32*
IDL apolipoprotein-B	7.22 (3.36 to 11.08)	2.63E-04	…	…	…
IDL cholesterol	7.03 (3.27 to 10.80)	2.68E-04	IDL cholesterol	2.36 (0.26 to 4.46)	2.79E-02
IDL free cholesterol	6.96 (3.17 to 10.76)	3.41E-04	IDL free cholesterol	0.10 (−1.97 to 2.18)	9.22E-01
IDL phospholipids	9.29 (5.47 to 13.11)	2.18E-06	IDL phospholipids	2.10 (0.04 to 4.16)	4.56E-02
IDL triglycerides	11.42 (7.59 to 15.25)	6.89E-09	IDL triglycerides	7.10 (5.50 to 8.70)	6.03E-18*
LDL triglycerides	6.68 (3.08 to 10.28)	2.89E-04	LDL triglycerides	5.59 (3.92 to 7.26)	6.52E-11*
LDL-3 free cholesterol	−8.34 (−12.35 to −4.34)	4.83E-05	…	…	…
LDL-5 triglycerides	6.56 (2.91 to 10.21)	4.46E-04	…	…	…
Total triglycerides	14.28 (10.60 to 17.96)	6.07E-14	Total triglycerides	11.10 (9.38 to 12.83)	1.90E-35*
VLDL apolipoprotein-B	12.48 (8.81 to 16.15)	4.37E-11	…	…	…
VLDL cholesterol	10.86 (7.21 to 14.52)	7.85E-09	VLDL cholesterol	8.77 (6.84 to 10.71)	1.22E-18*
VLDL free cholesterol	12.87 (9.20 to 16.54)	1.07E-11	…	…	…
VLDL phospholipids	13.43 (9.75 to 17.12)	1.76E-12	…	…	…
VLDL triglycerides	14.91 (11.21 to 18.61)	7.55E-15	VLDL triglycerides	11.39 (9.63 to 13.15)	8.09E-36*
XXL VLDL cholesterol	10.29 (6.41 to 14.16)	2.40E-07	XXL VLDL cholesterol	7.18 (4.65 to 9.71)	3.05E-08*
XXL VLDL free cholesterol	11.68 (7.97 to 15.39)	9.89E-10	XXL VLDL free cholesterol	8.09 (5.60 to 10.58)	2.34E-10*

Continued

Table 3. Continued

MESA			NEO Study		
Metabolite	Effect Estimate β (95% CI)	Nominal *P* Value	Metabolite	Effect Estimate β (95% CI)	Nominal *P* Value
XXL VLDL phospholipids	15.30 (11.63 to 18.96)	8.45E-16	XXL VLDL phospholipids	9.13 (6.10 to 12.15)	3.81E-09*
XXL VLDL triglycerides	16.17 (12.52 to 19.83)	1.78E-17	XXL VLDL triglycerides	9.37 (4.55 to 14.20)	1.43E-04*
Extralarge VLDL cholesterol	10.23 (6.59 to 13.87)	4.53E-08	Extralarge VLDL cholesterol	7.33 (4.57 to 10.09)	2.03E-07*
Extralarge VLDL free cholesterol	9.82 (6.11 to 13.52)	2.52E-07	Extralarge VLDL free cholesterol	7.31 (4.75 to 9.87)	2.28E-08*
Extralarge VLDL phospholipids	13.22 (9.56 to 16.88)	2.80E-12	Extralarge VLDL phospholipids	7.67 (4.39 to 10.94)	4.63E-06*
Extralarge VLDL triglycerides	12.92 (9.25 to 16.58)	8.77E-12	Extralarge VLDL triglycerides	9.04 (5.14 to 12.94)	5.87E-06*
Large VLDL cholesterol	10.34 (6.68 to 14.00)	4.00E-08	Large VLDL cholesterol	9.82 (7.84 to 11.79)	4.35E-22*
Large VLDL free cholesterol	10.58 (6.89 to 14.28)	2.51E-08	Large VLDL free cholesterol	9.82 (7.90 to 11.73)	2.50E-23*
Large VLDL phospholipids	11.85 (8.18 to 15.52)	3.75E-10	Large VLDL phospholipids	10.54 (8.55 to 12.53)	9.34E-25*
Large VLDL triglycerides	11.32 (7.65 to 14.98)	2.12E-09	Large VLDL triglycerides	11.24 (9.23 to 13.24)	2.21E-27*
Medium VLDL cholesterol	8.18 (4.60 to 11.75)	8.24E-06	Medium VLDL cholesterol	9.88 (7.95 to 11.81)	2.52E-23*
Medium VLDL free cholesterol	8.04 (4.42 to 11.67)	1.52E-05	Medium VLDL free cholesterol	10.99 (9.16 to 12.82)	3.37E-31*
Medium VLDL phospholipids	9.51 (5.89 to 13.13)	3.16E-07	Medium VLDL phospholipids	11.09 (9.28 to 12.90)	2.52E-32*
Medium VLDL triglycerides	10.08 (6.43 to 13.74)	8.02E-08	Medium VLDL triglycerides	11.39 (9.57 to 13.20)	1.07E-33*
Extrasmall VLDL cholesterol	−8.38 (−11.94 to −4.82)	4.58E-06	…	…	…
Extrasmall VLDL phospholipids	12.18 (8.55 to 15.82)	8.37E-11	Extrasmall VLDL phospholipids	4.62 (2.67 to 6.57)	3.53E-06*

Model adjusted for age, sex, race/ethnicity, socioeconomic status, smoking, physical activity, glucose and lipid-lowering medication use, and body mass index. Effect estimate β represents the difference in VAT area (in cm^2) per 1-SD in metabolite intensity (relative units). Lipoprotein particle subclasses range in size from extrasmall to XXL. HDL indicates high-density lipoprotein; IDL, intermediate-density lipoprotein; LDL, low-density lipoprotein; MESA, Multi-Ethnic Study of Atherosclerosis; NEO, Netherlands Epidemiology in Obesity; VAT, visceral adipose tissue; VLDL, very-LDL; XXL, very extralarge.
*Metabolites that were significant in the NEO study data set after false-discovery rate correction.

using the assessed genetic instruments linked to blood lipid levels.

Discussion

Using an untargeted metabolomics platform and a comprehensive pathway analysis tool in a large, multiethnic population cohort (MESA), we identified a metabolite signature associated with VAT linked to several putative biological pathways, including amino acid substrate use/metabolism and glycolysis/gluconeogenesis. We then replicated our findings in a separate epidemiological cohort (NEO study) using targeted metabolomics and found that acetylglycoproteins, branched-chain amino acids (isoleucine, leucine, and valine), glutamine (inversely), and serum triglycerides by ^{1}H NMR remained associated with VAT, even after adjustment for established surrogate biomarkers of VAT (BMI, fasting glucose, waist circumference, and serum triglycerides), suggesting that a single, fasting measurement of metabolites can provide biological information beyond standard risk markers of visceral fat. We believe these findings provide insight into potential mechanisms underpinning VAT metabolism distinct from generalized obesity (defined by BMI) and help to define a metabolic signature of visceral adiposity.

A growing number of studies have used targeted metabolic profiling as a tool for biomarker discovery in obesity, but studies to date have been composed of relatively small sample sizes[9,10] or histological samples of adipose tissue alone,[12] without targeting plasma-based metabolites that may be more easily obtained in clinical practice. Menni and colleagues[11] performed targeted metabolomics profiling of 208 plasma metabolites on 2401 women in the United Kingdom and assessed their relation to VAT measured by dual x-ray absorptiometry. They also observed associations between branched-chain amino acids, lactate, and VAT but did not perform replication studies to confirm their findings. Thus, one of the strengths of our investigation is the use of 2 well-characterized prospective cohorts, 1 for derivation and 1 for replication, each with dedicated imaging assessments of VAT, rather than relying on surrogate markers of VAT, such as anthropometric measurements. Furthermore, we use robust untargeted NMR-based experiments initially to broadly characterize the metabolic phenotype related to VAT and then replicate our findings using a targeted NMR approach in a

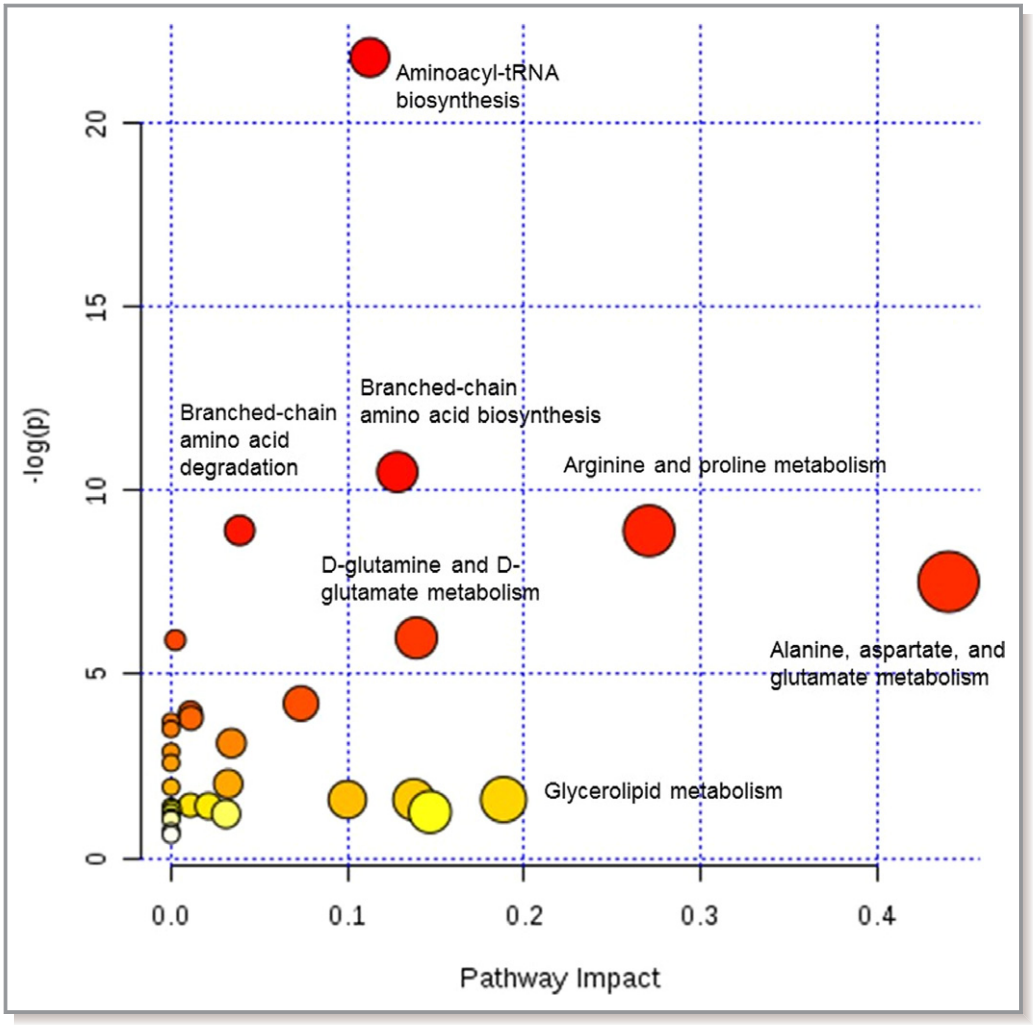

Figure 1. Targeted metabolomics pathway analysis in MESA (Multi-Ethnic Study of Atherosclerosis). Each node represents a separate biochemical pathway. The color of the node corresponds to its location on the *y* axis and indicates statistical significance in terms of -log(*P*) (higher values correspond to lower *P* values; eg, red nodes have low *P* values and yellow nodes have high *P* values). *P* values are derived from pathway enrichment analyses that measure the overall association of a set of metabolites that map to a particular pathway with the phenotype being examined (visceral adiposity). The size of the node corresponds to its location on the *x* axis and indicates to some extent the centrality of the metabolites in the data set for the represented pathway. This "pathway impact" measure combines theoretic measures to suggest whether the metabolites are critical connectors within a network as opposed to being more peripheral nodes. The total pathway impact for all metabolites in any given pathway from the metabolome databases (eg, Kyoto Encyclopedia of Genes and Genomes and Small Molecule Pathway databases) sum to 1. The pathway impact reported herein is the cumulative total of pathway impact for all metabolites used for analysis.

cohort that is well diversified demographically and geographically from the derivation cohort. All individuals in our study had assessments of BMI, waist circumference, and fasting glucose and triglycerides, allowing us to adjust for overall adiposity, glucose intolerance, and dyslipidemia.

Several limitations of the study merit comment. First, our findings should be primarily understood within a biological context; the utility of these metabolites for use in predictive modeling when added to standard clinical risk scores requires further study. Second, for MESA, because the metabolites were measured at a different time point than the abdominal imaging, we cannot exclude the possibility that metabolite concentrations might have differed at the follow-up examination. Different imaging methods were used to estimate VAT in each cohort; however, the imaging for both cohorts included the area around the fifth lumbar vertebrae, and multiple transverse cross-sectional slices were analyzed and averaged to obtain the final mean VAT value comparable between

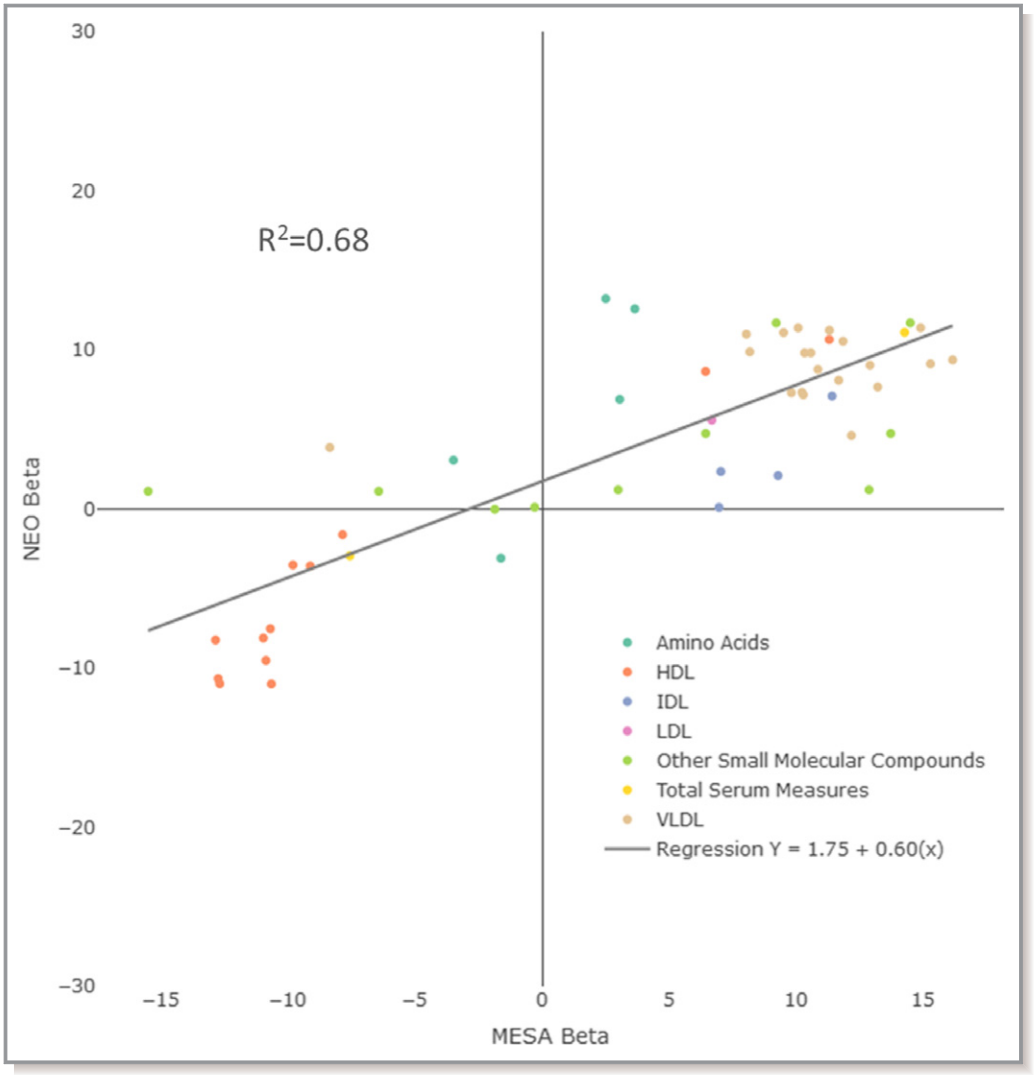

Figure 2. Associations between metabolites and visceral adipose tissue: correlation of the β coefficients between the 2 cohort studies. Scatterplot with regression line of β coefficients from each cohort study with each colored dot representing an individual metabolite. β Coefficients represent the difference in visceral adipose tissue area (in cm^2) per SD metabolite intensity and are from a model adjusted for age, sex, race/ethnicity, socioeconomic status, smoking, physical activity, glucose and lipid-lowering medication use, and body mass index. HDL indicates high-density lipoprotein; IDL, intermediate-density lipoprotein; LDL, low-density lipoprotein; MESA, Multi-Ethnic Study of Atherosclerosis; NEO, Netherlands Epidemiology in Obesity; VLDL, very-LDL.

cohorts. Furthermore, prior work showed good agreement (<3% difference in Bland-Altman analysis) between computed tomography and MRI for the measurement of VAT.[27] Although the cohorts varied both geographically and demographically, and metabolites in each cohort were measured using different algorithms, the replication observed across cohorts despite these differences in study populations (different amounts of VAT, different demographics, and different metabolomics platforms) makes our findings robust. However, it is possible that differences in ethnicity, diet, or distribution of obesity between the cohorts could partially explain the variability observed in metabolite associations in race-stratified analyses. These differences are likely most important for lipid metabolites given the known differences in lipid profiles between white and black individuals.[28] Furthermore, these differences may at least partially explain the observation that some metabolites found to be significant in MESA are not replicated in the NEO study. Moreover, we cannot generalize to other populations not well represented in either cohort in which alternative metabolite relationships may exist. Because our study was cross-sectional by design, we cannot comment on the relationship between temporal changes in metabolite levels and visceral fat. However, although the Mendelian randomization analyses did not demonstrate a causal

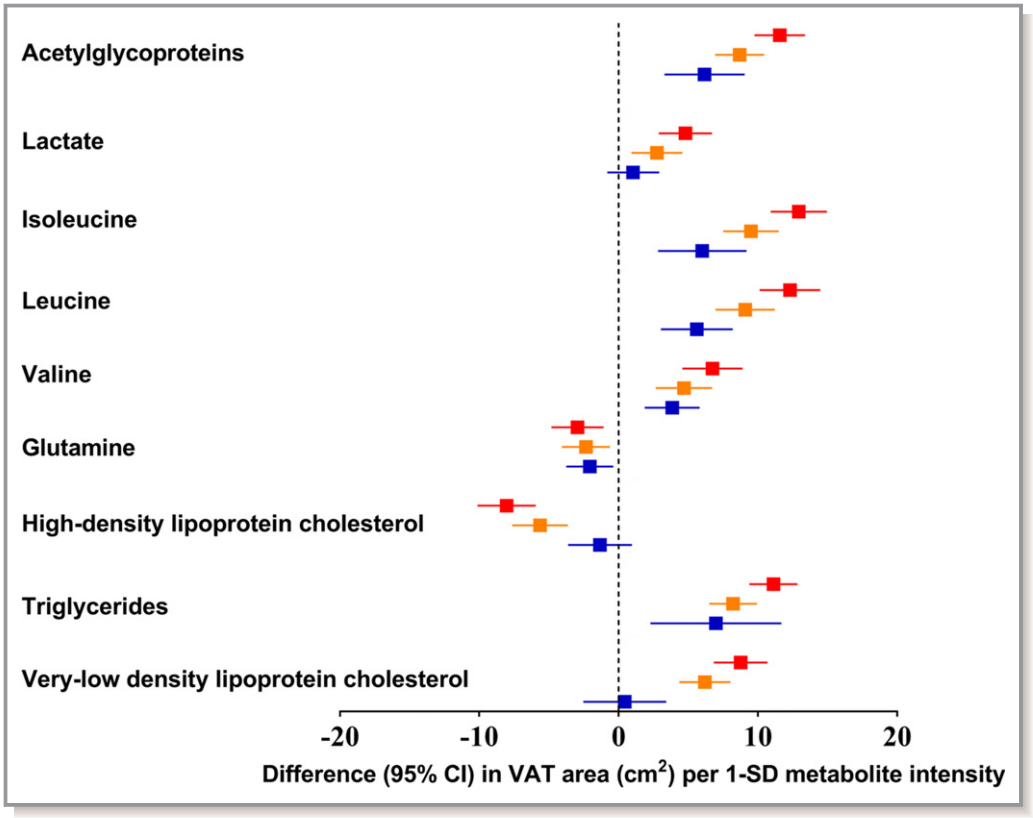

Figure 3. Associations between selected metabolites and visceral adiposity, adjusted for important metabolic phenotypes in the NEO (Netherlands Epidemiology in Obesity) study. Forest plot of associations between selected metabolites and visceral adipose tissue in the NEO study cohort. Each set of 3 nodes on the graph corresponds to a different metabolite. The first (red) node in each set represents the difference with 95% CI in visceral adipose tissue (VAT) area (in cm^2) per 1-SD metabolite intensity, adjusted for age, sex, race/ethnicity, socioeconomic status, smoking, physical activity, glucose and lipid-lowering medication use, and body mass index. The second (orange) node in each set represents the model additionally adjusted for fasting plasma glucose level and waist circumference, and the third (blue) node represents the model additionally adjusted for serum triglyceride level, measured by standard assay.

relationship between genetic instruments linked to blood lipid levels and VAT volume, a reverse directionality is more likely in that excess VAT may cause an atherogenic dyslipidemia. In line with the study by Xu et al,[29] because of the large differences in GWAS (genome-wide association study) sample size (n=322 154 for BMI, and n=18 832 for visceral fat), we cannot exclude that small causal effects of blood lipid concentrations on visceral fat may have been undetected. Further Mendelian randomization studies using genetic instruments linked to VAT will help elucidate the causal effects of VAT on metabolic traits. Finally, although we identified several biological pathways using metabolites associated with VAT, our interpretation of pathways must remain circumspect and hypothesis generating. In many instances, the identified metabolites represented substrates in the pathway rather than products, yielding one-sided evidence of biological relevance. Furthermore, the level of metabolomics detail derived with ^{1}H NMR is not sufficient to yield firm conclusions about the involvement of pathways.

Our findings, which highlight acetylglycoproteins, branched-chain amino acids, lactate, glutamine (inversely associated), and an atherogenic dyslipidemic profile (high triglycerides and VLDL and low HDL) from hundreds of metabolites assayed, are noteworthy in the context of experimental and clinical data suggesting that certain metabolites may be both markers and mediators of adverse health outcomes related to visceral obesity. For example, breakdown products of acetylglycoproteins, such as mannose, are elevated in individuals with insulin resistance[30] and associated with incident type 2 diabetes mellitus and CVD.[31] Indeed, we found that total acetylglycoproteins (and mannose in MESA) were significantly positively associated with VAT and that they remained associated with VAT even after adjustment for markers of glycemia and dyslipidemia in the NEO study. Acetylglycoproteins may perform a variety of cellular functions, including enzymatic catalysis, protein folding, conformation, and stabilization of biological membranes important for metabolic homeostasis[32]; perturbation of this highly

regulated system may increase circulating concentrations of acetylglycoproteins and represent a potential biomarker of visceral adiposity-related disease risk.

Glutamine, the most abundant free amino acid in human blood,[33] plays a role in a variety of biochemical functions and was inversely associated with VAT in our study. In prior work, urinary glutamine was inversely related to higher BMI and waist circumference in a population-based sample of adults.[10] Furthermore, plasma glutamine was inversely correlated with indexes of obesity and dysglycemia in healthy Japanese adults,[34] and a high plasma glutamine/glutamate ratio was associated with lower risk of incident diabetes mellitus in the FHS (Framingham Heart Study).[35] In experimental models, administration of glutamine in mice led to both improved glucose tolerance and lower blood pressure.[35] Therefore, in the context of these prior studies, our findings may indicate that visceral obesity reflects a relative "glutamine deficiency," representing dysmetabolic, dysfunctional adiposity with adverse cardiometabolic consequences.

Lactate is a by-product of anaerobic metabolism in cells when the energy-producing capacity of aerobic metabolism is exceeded or when oxygen is not available to participate in cellular respiration. There is substantial evidence, particularly from animal studies, that hypoxia develops in adipose tissue as the tissue mass expands, and the reduction in the oxygen content underlies an inflammatory response.[36] In hypoxic adipose tissue, secretion of multiple inflammation-related adipokines is upregulated, and there is a switch from oxidative metabolism to anaerobic glycolysis, with corresponding increases in lactate production.[37] The positive association between elevated lactate and VAT seen in our study may reflect the systemic effects of adipose tissue hypoxia, which are more common in VAT compared with other depots.[38] Alternatively, higher lactate, seen in our study, may reflect abnormal mitochondrial function.[39,40] Metabolic flux studies using biological tracers have shown that glucose feeds the tricarboxylic acid cycle (an integral component of oxidative phosphorylation in the electron transport chain in mitochondria) via circulating lactate and that circulatory turnover flux of lactate is the highest of all metabolites, exceeding that of glucose in mice.[41] Downregulation of several genes in the electron transport chain was found in viscerally obese women with diabetes mellitus and was, in part, mediated by expression of tumor necrosis factor-α, an important inflammatory cytokine implicated in the pathogenesis of type 2 diabetes mellitus.[42] A separate study also found that mitochondrial biogenesis and markers essential to aerobic metabolism were downregulated in acquired obesity in monozygotic twins.[43] Furthermore, studies of inborn errors of metabolism related to mitochondrial dysfunction have identified multiple metabolites downstream of primary mitochondrial lesions, including lactate and several amino acids.[44,45] Therefore, alterations in whole body mitochondrial oxidative phosphorylation capacity in multiple tissues, reflected by metabolomics disturbances, may contribute to a shared pathogenesis of VAT accumulation and cardiometabolic disease.

Branched-chain amino acids have been consistently linked to obesity and metabolic disease in recent years. Branched-chain amino acids are activators of the mammalian target of rapamycin signaling pathway, and high concentrations of these amino acids induce mammalian target of rapamycin hyperactivity, leading to impaired pancreatic β cell insulin secretion and insulin resistance.[46] Newgard and colleagues showed, in a rat model, that a dietary pattern of high-fat consumption with branched-chain amino acid supplementation led to obesity-associated insulin resistance via long-term activation of mammalian target of rapamycin that was reversed by the mammalian target of rapamycin inhibitor, rapamycin.[47] They also used principal components analysis to show that branched-chain amino acid concentrations can be used to differentiate metabolic signatures between obese and lean humans. Wang and colleagues further translated these findings to humans in the FHS by demonstrating that a branched-chain amino acid signature was associated with elevated BMI[48] and increased risk of type 2 diabetes mellitus.[8] However, they found considerable overlap in metabolic profiles between BMI, insulin resistance, and dyslipidemia. Indeed, many studies have found similar "metabolic profiles" associated with a broad range of diseases, from diabetes mellitus to CVD, suggesting that alterations in the metabolic processes reflected by these biomarkers may be more indicative of generalized metabolic derangements rather than markers of a specific disease.[49] Our findings may elucidate the reason for this metabolic overlap because excess visceral adiposity is a fundamental link between obesity and several adverse cardiometabolic traits.

It is well known that VAT is associated with an atherogenic, dyslipidemic lipid/lipoprotein profile, including high triglycerides, low HDL-C,[50,51] smaller LDL and HDL particle size, larger VLDL size, and increased LDL and VLDL particle number.[3] Indeed, in our study, HDL-C, larger HDL-related particles, and plasma apolipoprotein-A1 (a major protein component of HDL particles in plasma) were inversely associated with VAT, whereas triglycerides and VLDL-related particles were consistently positively associated with VAT (in both derivation and replication cohorts). Abnormalities in triglycerides and VLDL are more closely linked with entities classically related to VAT, such as the metabolic syndrome, insulin resistance, and the hypertriglyceridemic waist,[52,53] whereas alterations in HDL metabolism likely relate to atherogenesis through different mechanisms.[54,55] Therefore, our results may reflect multiple mechanistic pathways through which VAT and lipid/lipoproteins interact to influence cardiovascular and metabolic risk.

The ability to identify individuals before the onset of obesity-related complications is particularly important for

cardiometabolic diseases because therapies exist that can slow or prevent end-organ damage over time. Although anthropometric indexes of obesity (eg, BMI and waist circumference) are easy to implement clinically, their correlation with direct imaging-based assessments of visceral adiposity is modest; furthermore, these indexes incorporate both the abdominal subcutaneous and visceral depots that, as discussed, are anatomically and functionally distinct. Newer imaging-based methods offer more sensitivity and specificity for measuring VAT but have significant drawbacks, limiting their use in clinical practice. Blood-based metabolic profiling of VAT using a limited set of important metabolites may address this implementation gap between recognizing the role of visceral adiposity in cardiometabolic disease and actually assessing it clinically. Additional studies examining the relationship between metabolite signatures and future diabetes mellitus and/or cardiovascular events are an exciting next step in this field. Given that these new analyses would be more clinically oriented and require rigorous analytical approaches to evaluate the utility of metabolites in risk prediction for cardiometabolic events, they are beyond the scope of the current study.

In conclusion, from a panel of >30 000 metabolomics features, acetylglycoproteins, branched-chain amino acids, lactate, glutamine, and markers of atherogenic dyslipidemia emerged as strong markers of visceral adiposity. A single, fasting measurement of these metabolites may provide additional information over standard risk markers of visceral fat (BMI, fasting glucose, waist circumference, and serum triglycerides). Further investigation is warranted to determine whether NMR-based metabolic profiling can improve screening and detection of visceral adiposity beyond simple anthropometric measures and the hypertriglyceridemic waist to help identify appropriate candidates for interventions and reduce the cardiometabolic complications of visceral obesity.

Acknowledgments

The authors thank the investigators, staff, and participants of MESA (Multi-Ethnic Study of Atherosclerosis) for their valuable contributions. A full list of participating MESA investigators and institutions can be found at http://www.mesa-nhlbi.org. We express our gratitude to all participants of the NEO (Netherlands Epidemiology in Obesity) study, in addition to all participating general practitioners. We furthermore thank P. R. van Beelen and all research nurses for collecting the data, P. J. Noordijk and her team for sample handling and storage, and I. de Jonge for data management.

Sources of Funding

Dr Neeland is supported by grant K23 DK106520 from the National Institutes of Health (NIH) and by the Dedman Family Scholarship in Clinical Care from the University of Texas Southwestern. MESA (Multi-Ethnic Study of Atherosclerosis) was supported by contracts HHSN268201500003I, N01-HC-95159, N01-HC-95160, N01-HC-95161, N01-HC-95162, N01-HC-95163, N01-HC-95164, N01-HC-95165, N01-HC-95166, N01-HC-95167, N01-HC-95168, and N01-HC-95169 from the National Heart, Lung, and Blood Institute (NHLBI); and by grants UL1-TR-000040, UL1-TR-001079, and UL1-TR-001420 from the National Center for Advancing Translational Sciences. Dr Allison was supported by funding for MESA Abdominal Body Composition Ancillary study from the NHLBI (R01-HL088451). Dr Karaman acknowledges support from the European Union PhenoMeNal Project (Horizon 2020, 654241). The Development of Combinatorial Biomarkers for Subclinical Atherosclerosis project was supported by a grant from the European Union Seventh Framework Programme (305422). The NEO (Netherlands Epidemiology in Obesity) study is supported by the participating departments, the division, and the Board of Directors of the Leiden University Medical Center, and by the Leiden University, Research Profile Area "Vascular and Regenerative Medicine." We acknowledge support from the Netherlands Cardiovascular Research Initiative: an initiative with support of the Dutch Heart Foundation (CVON2014-02 ENERGISE). Dr Mook-Kanamori is supported by the Dutch Science Organization (ZonMW-VENI Grant 916.14.023). The content is solely the responsibility of the authors and does not necessarily represent the official views of the NIH.

Disclosures

Dr Neeland has received honoraria, consulting and speaker's bureau fees, and travel support from Boehringer-Ingelheim/Lilly Alliance (significant), has received a research grant from Novo Nordisk (significant), and is a member of the scientific advisory board of AMRA Medical (modest). The remaining authors have no disclosures to report.

References

1. Wildman RP, Muntner P, Reynolds K, McGinn AP, Rajpathak S, Wylie-Rosett J, Sowers MR. The obese without cardiometabolic risk factor clustering and the normal weight with cardiometabolic risk factor clustering: prevalence and correlates of 2 phenotypes among the US population (NHANES 1999–2004). *Arch Intern Med*. 2008;168:1617–1624.
2. Cornier MA, Despres JP, Davis N, Grossniklaus DA, Klein S, Lamarche B, Lopez-Jimenez F, Rao G, St-Onge MP, Towfighi A, Poirier P. Assessing adiposity: a scientific statement from the American Heart Association. *Circulation*. 2011;124:1996–2019.
3. Neeland IJ, Ayers CR, Rohatgi AK, Turer AT, Berry JD, Das SR, Vega GL, Khera A, McGuire DK, Grundy SM, de Lemos JA. Associations of visceral and abdominal subcutaneous adipose tissue with markers of cardiac and metabolic risk in obese adults. *Obesity (Silver Spring)*. 2013;21:E439–E447.
4. Neeland IJ, Turer AT, Ayers CR, Powell-Wiley TM, Vega GL, Farzaneh-Far R, Grundy SM, Khera A, McGuire DK, de Lemos JA. Dysfunctional adiposity and the risk of prediabetes and type 2 diabetes in obese adults. *JAMA*. 2012;308:1150–1159.
5. Shah RV, Murthy VL, Abbasi SA, Blankstein R, Kwong RY, Goldfine AB, Jerosch-Herold M, Lima JA, Ding J, Allison MA. Visceral adiposity and the risk of

metabolic syndrome across body mass index: the MESA Study. *JACC Cardiovasc Imaging*. 2014;7:1221–1235.

6. de Mutsert R, Gast K, Widya R, de Koning E, Jazet I, Lamb H, le Cessie S, de Roos A, Smit J, Rosendaal F, den Heijer M. Associations of abdominal subcutaneous and visceral fat with insulin resistance and secretion differ between men and women: the Netherlands Epidemiology of Obesity study. *Metab Syndr Relat Disord*. 2018;16:54–63.
7. Tzoulaki I, Ebbels TM, Valdes A, Elliott P, Ioannidis JP. Design and analysis of metabolomics studies in epidemiologic research: a primer on -omic technologies. *Am J Epidemiol*. 2014;180:129–139.
8. Wang TJ, Larson MG, Vasan RS, Cheng S, Rhee EP, McCabe E, Lewis GD, Fox CS, Jacques PF, Fernandez C, O'Donnell CJ, Carr SA, Mootha VK, Florez JC, Souza A, Melander O, Clish CB, Gerszten RE. Metabolite profiles and the risk of developing diabetes. *Nat Med*. 2011;17:448–453.
9. Martin FP, Montoliu I, Collino S, Scherer M, Guy P, Tavazzi I, Thorimbert A, Moco S, Rothney MP, Ergun DL, Beaumont M, Ginty F, Qanadli SD, Favre L, Giusti V, Rezzi S. Topographical body fat distribution links to amino acid and lipid metabolism in healthy obese women [corrected]. *PLoS One*. 2013;8:e73445.
10. Schlecht I, Gronwald W, Behrens G, Baumeister SE, Hertel J, Hochrein J, Zacharias HU, Fischer B, Oefner PJ, Leitzmann MF. Visceral adipose tissue but not subcutaneous adipose tissue is associated with urine and serum metabolites. *PLoS One*. 2017;12:e0175133.
11. Menni C, Migaud M, Glastonbury CA, Beaumont M, Nikolaou A, Small KS, Brosnan MJ, Mohney RP, Spector TD, Valdes AM. Metabolomic profiling to dissect the role of visceral fat in cardiometabolic health. *Obesity (Silver Spring)*. 2016;24:1380–1388.
12. Hanzu FA, Vinaixa M, Papageorgiou A, Parrizas M, Correig X, Delgado S, Carmona F, Samino S, Vidal J, Gomis R. Obesity rather than regional fat depots marks the metabolomic pattern of adipose tissue: an untargeted metabolomic approach. *Obesity (Silver Spring)*. 2014;22:698–704.
13. Bild DE, Bluemke DA, Burke GL, Detrano R, Diez Roux AV, Folsom AR, Greenland P, Jacob DR Jr, Kronmal R, Liu K, Nelson JC, O'Leary D, Saad MF, Shea S, Szklo M, Tracy RP. Multi-Ethnic Study of Atherosclerosis: objectives and design. *Am J Epidemiol*. 2002;156:871–881.
14. Yeboah J, Bertoni AG, Herrington DM, Post WS, Burke GL. Impaired fasting glucose and the risk of incident diabetes mellitus and cardiovascular events in an adult population: MESA (Multi-Ethnic Study of Atherosclerosis). *J Am Coll Cardiol*. 2011;58:140–146.
15. Ainsworth BE, Haskell WL, Whitt MC, Irwin ML, Swartz AM, Strath SJ, O'Brien WL, Bassett DR Jr, Schmitz KH, Emplaincourt PO, Jacobs DR Jr, Leon AS. Compendium of physical activities: an update of activity codes and MET intensities. *Med Sci Sports Exerc*. 2000;32:S498–S504.
16. De Mutsert R, Den Heijer M, Rabelink TJ, Smit JWA, Romijn JA, Jukema JW, De Roos A, Cobbaert CM, Kloppenburg M, Le Cessie S, Middeldorp S, Rosendaal FR. The Netherlands Epidemiology of Obesity (NEO) study: study design and data collection. *Eur J Epidemiol*. 2013;28:513–523.
17. Korn EL, Graubard BI. Epidemiologic studies utilizing surveys: accounting for the sampling design. *Am J Public Health*. 1991;81:1166–1173.
18. Dona AC, Jimenez B, Schafer H, Humpfer E, Spraul M, Lewis MR, Pearce JT, Holmes E, Lindon JC, Nicholson JK. Precision high-throughput proton NMR spectroscopy of human urine, serum, and plasma for large-scale metabolic phenotyping. *Anal Chem*. 2014;86:9887–9894.
19. Petersen M, Dyrby M, Toubro S, Engelsen SB, Norgaard L, Pedersen HT, Dyerberg J. Quantification of lipoprotein subclasses by proton nuclear magnetic resonance-based partial least-squares regression models. *Clin Chem*. 2005;51:1457–1461.
20. Karaman I, Ferreira DL, Boulange CL, Kaluarachchi MR, Herrington D, Dona AC, Castagne R, Moayyeri A, Lehne B, Loh M, de Vries PS, Dehghan A, Franco OH, Hofman A, Evangelou E, Tzoulaki I, Elliott P, Lindon JC, Ebbels TM. Workflow for integrated processing of multicohort untargeted 1H NMR metabolomics data in large-scale metabolic epidemiology. *J Proteome Res*. 2016;15:4188–4194.
21. Soininen P, Kangas AJ, Wurtz P, Suna T, Ala-Korpela M. Quantitative serum nuclear magnetic resonance metabolomics in cardiovascular epidemiology and genetics. *Circ Cardiovasc Genet*. 2015;8:192–206.
22. Kettunen J, Demirkan A, Wurtz P, Draisma HH, Haller T, Rawal R, Vaarhorst A, Kangas AJ, Lyytikainen LP, Pirinen M, Pool R, Sarin AP, Soininen P, Tukiainen T, Wang Q, Tiainen M, Tynkkynen T, Amin N, Zeller T, Beekman M, Deelen J, van Dijk KW, Esko T, Hottenga JJ, van Leeuwen EM, Lehtimaki T, Mihailov E, Rose RJ, de Craen AJ, Gieger C, Kahonen M, Perola M, Blankenberg S, Savolainen MJ, Verhoeven A, Viikari J, Willemsen G, Boomsma DI, van Duijn CM, Eriksson J, Jula A, Jarvelin MR, Kaprio J, Metspalu A, Raitakari O, Salomaa V, Slagboom PE, Waldenberger M, Ripatti S, Ala-Korpela M. Genome-wide study for circulating metabolites identifies 62 loci and reveals novel systemic effects of LPA. *Nat Commun*. 2016;7:11122.
23. Holmes MV, Millwood IY, Kartsonaki C, Hill MR, Bennett DA, Boxall R, Guo Y, Xu X, Bian Z, Hu R, Walters RG, Chen J, Ala-Korpela M, Parish S, Clarke RJ, Peto R, Collins R, Li L, Chen Z; China Kadoorie Biobank Collaborative Group. Lipids, lipoproteins, and metabolites and risk of myocardial infarction and stroke. *J Am Coll Cardiol*. 2018;71:620–632.
24. Schweitzer L, Geisler C, Pourhassan M, Braun W, Gluer CC, Bosy-Westphal A, Muller MJ. What is the best reference site for a single MRI slice to assess whole-body skeletal muscle and adipose tissue volumes in healthy adults? *Am J Clin Nutr*. 2015;102:58–65.
25. Xia J, Wishart DS. Using MetaboAnalyst 3.0 for comprehensive metabolomics data analysis. *Curr Protoc Bioinformatics*. 2016;55:14.10.1–14.10.91.
26. Lemieux I, Pascot A, Couillard C, Lamarche B, Tchernof A, Almeras N, Bergeron J, Gaudet D, Tremblay G, Prud'homme D, Nadeau A, Despres JP. Hypertriglyceridemic waist: a marker of the atherogenic metabolic triad (hyperinsulinemia; hyperapolipoprotein B; small, dense LDL) in men? *Circulation*. 2000;102:179–184.
27. Klopfenstein BJ, Kim MS, Krisky CM, Szumowski J, Rooney WD, Purnell JQ. Comparison of 3 T MRI and CT for the measurement of visceral and subcutaneous adipose tissue in humans. *Br J Radiol*. 2012;85:e826–e830.
28. Chandra A, Neeland IJ, Das SR, Khera A, Turer AT, Ayers CR, McGuire DK, Rohatgi A. Relation of black race between high density lipoprotein cholesterol content, high density lipoprotein particles and coronary events (from the Dallas Heart Study). *Am J Cardiol*. 2015;115:890–894.
29. Xu L, Borges MC, Hemani G, Lawlor DA. The role of glycaemic and lipid risk factors in mediating the effect of BMI on coronary heart disease: a two-step, two-sample Mendelian randomisation study. *Diabetologia*. 2017;60:2210–2220.
30. Lee S, Zhang C, Kilicarslan M, Piening BD, Bjornson E, Hallstrom BM, Groen AK, Ferrannini E, Laakso M, Snyder M, Bluher M, Uhlen M, Nielsen J, Smith U, Serlie MJ, Boren J, Mardinoglu A. Integrated network analysis reveals an association between plasma mannose levels and insulin resistance. *Cell Metab*. 2016;24:172–184.
31. Mardinoglu A, Stancakova A, Lotta LA, Kuusisto J, Boren J, Bluher M, Wareham NJ, Ferrannini E, Groop PH, Laakso M, Langenberg C, Smith U. Plasma mannose levels are associated with incident type 2 diabetes and cardiovascular disease. *Cell Metab*. 2017;26:281–283.
32. Bermingham ML, Colombo M, McGurnaghan SJ, Blackbourn LAK, Vuckovic F, Pucic Bakovic M, Trbojevic-Akmacic I, Lauc G, Agakov F, Agakova AS, Hayward C, Klaric L, Palmer CNA, Petrie JR, Chalmers J, Collier A, Green F, Lindsay RS, Macrury S, McKnight JA, Patrick AW, Thekkepat S, Gornik O, McKeigue PM, Colhoun HM; SDRN Type 1 Bioresource Investigators. N-glycan profile and kidney disease in type 1 diabetes. *Diabetes Care*. 2018;41:79–87.
33. Brosnan JT. Interorgan amino acid transport and its regulation. *J Nutr*. 2003;133:2068S–2072S.
34. Takashina C, Tsujino I, Watanabe T, Sakaue S, Ikeda D, Yamada A, Sato T, Ohira H, Otsuka Y, Oyama-Manabe N, Ito YM, Nishimura M. Associations among the plasma amino acid profile, obesity, and glucose metabolism in Japanese adults with normal glucose tolerance. *Nutr Metab (Lond)*. 2016;13:5.
35. Cheng S, Rhee EP, Larson MG, Lewis GD, McCabe EL, Shen D, Palma MJ, Roberts LD, Dejam A, Souza AL, Deik AA, Magnusson M, Fox CS, O'Donnell CJ, Vasan RS, Melander O, Clish CB, Gerszten RE, Wang TJ. Metabolite profiling identifies pathways associated with metabolic risk in humans. *Circulation*. 2012;125:2222–2231.
36. Engin A. Adipose tissue hypoxia in obesity and its impact on preadipocytes and macrophages: hypoxia hypothesis. *Adv Exp Med Biol*. 2017;960:305–326.
37. Trayhurn P. Hypoxia and adipose tissue function and dysfunction in obesity. *Physiol Rev*. 2013;93:1–21.
38. Revelo XS, Luck H, Winer S, Winer DA. Morphological and inflammatory changes in visceral adipose tissue during obesity. *Endocr Pathol*. 2014;25:93–101.
39. Crescenzo R, Bianco F, Mazzoli A, Giacco A, Liverini G, Iossa S. A possible link between hepatic mitochondrial dysfunction and diet-induced insulin resistance. *Eur J Nutr*. 2016;55:1–6.
40. Kim JA, Wei Y, Sowers JR. Role of mitochondrial dysfunction in insulin resistance. *Circ Res*. 2008;102:401–414.
41. Hui S, Ghergurovich JM, Morscher RJ, Jang C, Teng X, Lu W, Esparza LA, Reya T, Le Z, Yanxiang Guo J, White E, Rabinowitz JD. Glucose feeds the TCA cycle via circulating lactate. *Nature*. 2017;551:115–118.
42. Dahlman I, Forsgren M, Sjogren A, Nordstrom EA, Kaaman M, Naslund E, Attersand A, Arner P. Downregulation of electron transport chain genes in visceral adipose tissue in type 2 diabetes independent of obesity and possibly involving tumor necrosis factor-alpha. *Diabetes*. 2006;55:1792–1799.
43. Heinonen S, Buzkova J, Muniandy M, Kaksonen R, Ollikainen M, Ismail K, Hakkarainen A, Lundbom J, Lundbom N, Vuolteenaho K, Moilanen E, Kaprio J,

Rissanen A, Suomalainen A, Pietilainen KH. Impaired mitochondrial biogenesis in adipose tissue in acquired obesity. *Diabetes*. 2015;64:3135–3145.

44. Thompson Legault J, Strittmatter L, Tardif J, Sharma R, Tremblay-Vaillancourt V, Aubut C, Boucher G, Clish CB, Cyr D, Daneault C, Waters PJ; LSFC Consortium, Vachon L, Morin C, Laprise C, Rioux JD, Mootha VK, Des Rosiers C. A metabolic signature of mitochondrial dysfunction revealed through a monogenic form of leigh syndrome. *Cell Rep*. 2015;13:981–989.
45. Shaham O, Slate NG, Goldberger O, Xu Q, Ramanathan A, Souza AL, Clish CB, Sims KB, Mootha VK. A plasma signature of human mitochondrial disease revealed through metabolic profiling of spent media from cultured muscle cells. *Proc Natl Acad Sci USA*. 2010;107:1571–1575.
46. Melnik BC. Leucine signaling in the pathogenesis of type 2 diabetes and obesity. *World J Diabetes*. 2012;3:38–53.
47. Newgard CB, An J, Bain JR, Muehlbauer MJ, Stevens RD, Lien LF, Haqq AM, Shah SH, Arlotto M, Slentz CA, Rochon J, Gallup D, Ilkayeva O, Wenner BR, Yancy WS Jr, Eisenson H, Musante G, Surwit RS, Millington DS, Butler MD, Svetkey LP. A branched-chain amino acid-related metabolic signature that differentiates obese and lean humans and contributes to insulin resistance. *Cell Metab*. 2009;9:311–326.
48. Ho JE, Larson MG, Ghorbani A, Cheng S, Chen MH, Keyes M, Rhee EP, Clish CB, Vasan RS, Gerszten RE, Wang TJ. Metabolomic profiles of body mass index in the Framingham Heart Study reveal distinct cardiometabolic phenotypes. *PLoS One*. 2016;11:e0148361.
49. Shah SH, Kraus WE, Newgard CB. Metabolomic profiling for the identification of novel biomarkers and mechanisms related to common cardiovascular diseases: form and function. *Circulation*. 2012;126:1110–1120.
50. Despres JP, Moorjani S, Ferland M, Tremblay A, Lupien PJ, Nadeau A, Pinault S, Theriault G, Bouchard C. Adipose tissue distribution and plasma lipoprotein levels in obese women: importance of intra-abdominal fat. *Arteriosclerosis*. 1989;9:203–210.
51. Despres JP, Moorjani S, Lupien PJ, Tremblay A, Nadeau A, Bouchard C. Regional distribution of body fat, plasma lipoproteins, and cardiovascular disease. *Arteriosclerosis*. 1990;10:497–511.
52. Sperling LS, Mechanick JI, Neeland IJ, Herrick CJ, Despres JP, Ndumele CE, Vijayaraghavan K, Handelsman Y, Puckrein GA, Araneta MR, Blum QK, Collins KK, Cook S, Dhurandhar NV, Dixon DL, Egan BM, Ferdinand DP, Herman LM, Hessen SE, Jacobson TA, Pate RR, Ratner RE, Brinton EA, Forker AD, Ritzenthaler LL, Grundy SM. The cardiometabolic health alliance: working toward a new care model for the metabolic syndrome. *J Am Coll Cardiol*. 2015;66:1050–1067.
53. Wajchenberg BL, Giannella-Neto D, da Silva ME, Santos RF. Depot-specific hormonal characteristics of subcutaneous and visceral adipose tissue and their relation to the metabolic syndrome. *Horm Metab Res*. 2002;34:616–621.
54. Link JJ, Rohatgi A, de Lemos JA. HDL cholesterol: physiology, pathophysiology, and management. *Curr Probl Cardiol*. 2007;32:268–314.
55. Rohatgi A, de Lemos JA, Shaul PW. HDL cholesterol efflux capacity and cardiovascular events. *N Engl J Med*. 2015;372:1871–1872.

Supplemental Material

Data S1.

Supplemental Methods

Preparation of samples, including quality controls (QCs)

The MESA samples were analyzed in two phases as part of EU-funded COMBI-BIO project along with samples from two other cohorts: The London Life Sciences Prospective Population[1] (LOLIPOP) and The Rotterdam Study[2]. Study samples were shipped on dry ice and stored at -80 C upon arrival until NMR analysis. Two types of QC samples were used to monitor the quality of the NMR data. One type (QC1) was a commercially available serum (human serum, off the clot, type AB, VWR catalog number BCHRS01049.2-01, VWR International Ltd, UK) and the other type (QC2) was prepared by pooling 50 µl aliquots of the phase 1 LOLIPOP samples. The QCs were aliquoted in 350 µl lots and stored at -80 °C. On the day of analysis, both QC and study samples were thawed and 300 µl of each sample was mixed with 300 µl of phosphate buffer ($NaHPO_4$, 0.075M, pH=7.4, as described previously[3]) in Eppendorfs for the phase 1 analysis, and in 96 well plates for the phase 2 analysis. After centrifugation (12,000 g at 4 °C for 5 minutes), 550 µl of each sample-buffer mixture was manually transferred into SampleJet 5 mm diameter NMR tubes and kept at 4 °C until analysis. In phase 1 one QC1 sample was incorporated in each 96 tube rack. In phase 2, a single QC2 sample was run in each 96 well plate, and a single QC1 sample was run every two plates. The coefficient of variation (CV, %), calculated as the standard deviation/mean concentration per metabolite * 100%, for both standard 1D NMR and CPMG acquisitions are listed in the table below.

	MESA
Metabolite	Coefficient of variation (%)
1D NMR	
Acetylglycoproteins	**2.08**
Choline	14.26
Creatinine	2.26
Glycerol	2.45
Glyceryl groups of lipids	1.36
Lactate	**5.91**
Mannose	6.55
Myo-inositol	0.63
Proline	0.83
Carr-Purcell-Meiboom-Gill Echo Acquisition (CPMG)	
2-Ketoisovalerate	5.61
Acetylglycoproteins	**4.69**
Alanine	8.55
Albumin	9.30
alpha-Glucose	6.75
Arginine	12.41
beta-Glucose	12.11
Choline	9.29
Citrate	41.50
Creatinine	13.07
Ornithine	35.98
Glutamate	28.45
Glutamine	**9.68**
Glyceryl groups of lipids	18.14
Isoleucine	**6.42**

Lactate	**8.49**
Leucine	**4.03**
Lysine	17.77
Mannose	8.47
Proline	7.19
Pyroglutamate	12.41
Valine	**12.01**

Metabolites in **bold** were significant in the NEO dataset after FDR correction

NMR data acquisition

Serum samples were prepared according to the Bruker standard method.[4] A standard ^{1}H NMR one-dimensional (1D NMR) spectrum with water suppression (also called the NOESY-presat sequence) and a T2-edited spectrum using the CPMG sequence were obtained for each sample. The standard ^{1}H NMR spectrum detects the peaks of all proton-containing compounds and as such the resultant spectrum comprises sharp peaks for small molecule species, broad bands from the lipoproteins and a largely featureless-background from proteins. The CPMG experiment exploits the variation in the nuclear spin relaxation times of the large and small molecules to reduce the broad signals from the large compounds (proteins and lipoproteins) producing a spectrum with a flatter baseline and mainly small molecule metabolite peaks. ^{1}H NMR spectra were acquired on a Bruker Ascend spectrometer (Bruker Biospin, Rheinstetten, Germany) operating at 600 MHz and equipped with a Bruker Advance III console. 32 scans were collected into 131,072 frequency domain points and a line broadening of 0.3 Hz was applied. The spectral processing was performed using the software TOPSPIN 3.1 (Bruker Biospin, Rheinstetten, Germany). For each spectrum, the free induction decay underwent a zero filling by a factor of two and a line broadening of 0.3 Hz producing 128K frequency domain points prior to Fourier

transformation. The spectra were then automatically phased and baseline corrected and the chemical shifts were calibrated to the glucose signal at 5.233 ppm. Spectral data were imported into MATLAB (Version 8.3 (R2014a) Mathworks Inc., Natick, MA, USA) for further processing. The ^{1}H NMR spectroscopic analysis was completed in six batches corresponding to the three cohorts and two ^{1}H NMR experimental phases. The processing workflow to integrate the multi-cohort ^{1}H NMR metabolic profiling data has been previously described.[5]

^{1}H NMR Lipoprotein profiles using Bruker lipoprotein subclass analysis

The Bruker lipoprotein subclass analysis was applied to the MESA cohort data. The quantification of the lipoprotein subclasses is based on the deconvolution of the methyl peak in the standard NMR spectrum near 0.89 ppm using a Bruker (Bruker Biospin, Rheinstetten, Germany) proprietary procedure adapted from Petersen et al.[6] To assess the measurement quality, the correlation coefficients between conventional measurements and the Bruker ^{1}H NMR-derived values of total HDL, LDL and triglycerides were calculated. Analysis of 105 lipoprotein subclasses was carried out including different chemical components of IDL (density 1.006-1.019 kg/L), VLDL (0.950-1.006 kg/L), LDL (density 1.09-1.63 kg/L) and HDL (density 1.063-1.210 kg/L). The LDL sub-fraction was fractionated into six density classes (LDL-1 1.019-1.031 kg/L, LDL-2 1.031-1.034 kg/L, LDL-3 1.034-1.037 kg/L, LDL-4 1.037-1.040 kg/L, LDL-5 1.040-1.044 kg/L, LDL-6 1.044-1.063 kg/L) and the HDL sub-fraction in four density classes (HDL-1 1.063-1.100 kg/L, HDL-2 1.100-1.125 kg/L, HDL-3 1.125-1.175 kg/L, HDL-4 1.175-1.210 kg/L).[6, 7]

Metabolite identification

To help with identification of peaks in the ^{1}H NMR data, reduction using a semi-automatic clustering of the full resolution ^{1}H NMR spectrum (30,590 features) was performed using the Statistical Recoupling of Variables (SRV).[8] The algorithm defines a cluster if 10 or more consecutive variables are correlated with each other, with a correlation threshold of r=0.9; clusters could also be grouped into a supercluster if the correlation with the neighbouring cluster was r=0.9 or above. To optimise the efficiency of SRV, superclusters were generated from the aggregation of a maximum of three clusters according to Blaise et al.[9] Each cluster was then manually checked to improve the groupings and identify peak overlaps. Thus, 132 clusters were identified in ^{1}H NMR standard 1D and 157 clusters in CPMG data, each of them corresponding to a single peak or a group or peaks.

The chemical shift (in ppm), the coupling constant value (J in Hz), the peak multiplicity (singlet, doublet, multiplet) and peak connectivity of the NMR signals of interest were identified using 1D and 2D (2D JRES, COrrelation SpectroscopY (COSY), TOtal Correlation SpectroscopY (TOCSY), Heteronuclear single quantum correlation spectroscopy (HSQC), the Human Metabolome Database) NMR experiments and statistical correlation methods (STOCSY (Statistical Total Correlation Spectroscopy), STORM (Subset Optimisation by Reference Matching)).[9-11] This information was then compared with available in-house and publicly available databases (Human Metabolome Database[12]) as well as with published works on human serum and plasma metabolite components. The metabolite identities were confirmed by spike-in experiments when the chemical standards were available. The level of peak overlap in the clusters of interest and the level of confidence in the assignment of the identified metabolites were adapted from Sumner et al.[13] The metabolite assignment is as follows – 1: Compound

identified with spiking, 2: Annotated compounds (without chemical reference standards, based upon physicochemical properties and/or spectral similarity with public/commercial spectral libraries), 3: Putatively characterized compound classes (e.g. based upon characteristic physicochemical properties of a chemical class of compounds, or by spectral similarity to known compounds of a chemical class) 4: Unknown compounds. a: well-resolved peaks which can be differentiated and quantified based upon spectral data. b: Overlapped or low-resolved peaks, from which signal differentiation and quantification may be compromised.

Metaboanalyst – a comprehensive tool for metabolomics analysis and interpretation

The pathway analysis in MetaboAnalyst is a free, web-based tool targeting for metabolomics data analysis. It uses the high-quality KEGG metabolic pathways as the backend knowledgebase. It integrates many well-established (i.e. univariate analysis, over-representation analysis) methods, as well as novel algorithms/concepts (GlobalTest, GlobalAncova, pathway topology analysis) into pathway analysis. In addition, MetPA implements a Google-Map style interactive visualization system to help users understand their analysis results.

Over-representation analysis is to test if a particular group of compounds is represented more than expected by chance within the user uploaded compound list. In the context of pathway analysis, we are testing if compounds involved in a particular pathway is enriched compared by random hits. The most common methods for such analysis is Fishers' exact test and hypergeometric test. Please note, the over-representation analysis only consider the count (i.e. the total number of compounds that match a particular pathway) and does not consider the

magnitude of their concentration changes (not quantitative). So compound that are changed more significant will be treated the same as compounds that are less significant.

Pathway enrichment analysis usually refers to quantitative enrichment analysis directly based on the compound concentration values as compared to the compound lists used by over representation analysis. It is usually more sensitive than over-representation analysis and has the potential to discover "subtle but consistent" changes among compounds within the same biological pathway. The program uses GlobalTest and GlobalAncova for pathway enrichment analysis when users upload concentration tables. Some important features about these two methods include that they support binary, multi-group, as well as continuous phenotypes, and p values can be approximated efficiently based on the asymptotic distribution without using permutations, which is critical for developing web applications.

The structure of biological pathways represents our knowledge about the complex relationships between molecules (activation, inhibition, reaction, etc.). However, neither over-representation analysis or pathway enrichment analysis take the pathway structure into consideration when determining which pathways are more likely to be involved in the conditions under study. It is obvious that changes in the key positions of a network will trigger more severe impact on the pathway than changes on marginal or relatively isolated positions. The program uses two well-established node centrality measures to estimate node importance - betweenness centrality and degree centrality. The former focus on node relative to overall pathway structure, while the latter focus on immediate local connectivities.

Mendelian Randomization Study of Genetic Traits Linked to Blood Lipid Levels and Visceral Adiposity

We selected uncorrelated genetic instruments previously found to associate with one or more lipid traits (high-density lipoprotein cholesterol (HDL-C, n=89), low-density lipoprotein cholesterol (LDL-C, n=80), and triglycerides (TG, n=54)) at a genome-wide significant level ($p<5x10^{-8}$) in the largest genome-wide meta-analysis of blood lipid levels to date.[14] This study included up to 188,577 European-ancestry individuals and estimated the additive effect of each genetic variant on blood lipid levels. We subsequently queried a large-scale genome-wide meta-analysis of ectopic fat depots for each genetic instruments' effect on visceral adipose tissue (VAT) volume.[15] This multiethnic meta-analysis included up to 18,332 individuals (18.9% African-descent, remainder European-descent) for the analyses on VAT volume and was conducted using a weighted z-score based approach, meaning that studies only contributed test statistics (z-scores). We therefore approximated beta coefficients and standard errors from the z-scores, effect allele frequencies, and sample sizes using a previously published method.[16] As effect allele frequencies were not provided in the publicly available summary statistics of the VAT volume analyses (downloaded from the NHLBI GRASP catalog[17], Build 2.0.0.0, https://grasp.nhlbi.nih.gov/), we utilized 1000 genomes phase 1 version 3 European population-specific allele frequencies as given in the legend files on the IMPUTE program website (https://mathgen.stats.ox.ac.uk/impute/impute.html). Whilst harmonizing the datasets we excluded palindromic genetic variants with intermediate minor allele frequencies (above 0.42) to avoid effect allele coding errors. Of the thirteen studies contributing to the genome-wide meta-analysis on VAT volume, four also contributed to the meta-analysis involving blood lipids levels. With respect to the larger dataset, up to 3.7% of overlap in participants may therefore

exist. However, given the strength of the genetic instruments, this overlap is unlikely to introduce noticeable bias into the analysis.[18]

For each set of genetic instruments (HDL-C, LDL-C, TG) we estimated the causal effect of blood lipid level on VAT volume by performing an inverse-variance weighted (IVW) linear regression of instrument-outcome associations on instrument-exposure associations, with the intercept constrained to zero.[19] As the instrument-outcome associations were constructed from z-scores, these associations and consequently also the causal effect estimators do not have interpretable units. However, these estimators can provide insight into the direction of association and provide a probability value indicative of the strength of the statistical evidence for an association.[16] We additionally performed three complementary sensitivity analyses which aim to provide asymptotically consistent causal estimates whilst relaxing the requirement of no horizontal pleiotropy amongst the genetic variants. First, the MR-Egger approach, of which the slope is an estimate of the causal effect and the intercept provides a formal test whether the average pleiotropic effect over the variants differs significantly from zero.[20] This approach assumes that the association of each genetic variant with the exposure is independent of the pleiotropic effect of the variant. Secondly, the weighted median estimator, which is consistent even when up to 50% of the weight in the analysis comes from invalid instruments.[21] Finally, the weighted mode-based estimator (MBE), which is consistent if the most common value of pleiotropy across the instruments is zero.[22] In addition, we provide funnel plots which display the causal estimate (i.e. Wald ratio) of each individual genetic variant against their precision. Asymmetric plots may be indicative of the presence of directional (i.e. unbalanced) pleiotropy.[20] Instruments were selected and all analyses were performed in R version 3.4.2[23] using the TwoSampleMR R-package which accompanies the MR-base analytical platform.[24]

Table S1. Metabolomics Biomarkers Measured in the NEO Study.

Abbreviation	Name	Unit
XL-HDL-P	Concentration of very large HDL particles	mol/L
XL-HDL-L	Total lipids in very large HDL	mmol/L
XL-HDL-PL	Phospholipids in very large HDL	mmol/L
XL-HDL-C	Total cholesterol in very large HDL	mmol/L
XL-HDL-CE	Cholesterol esters in very large HDL	mmol/L
XL-HDL-FC	Free cholesterol in very large HDL	mmol/L
XL-HDL-TG	Triglycerides in very large HDL	mmol/L
L-HDL-P	Concentration of large HDL particles	mol/L
L-HDL-L	Total lipids in large HDL	mmol/L
L-HDL-PL	Phospholipids in large HDL	mmol/L
L-HDL-C	Total cholesterol in large HDL	mmol/L
L-HDL-CE	Cholesterol esters in large HDL	mmol/L
L-HDL-FC	Free cholesterol in large HDL	mmol/L
L-HDL-TG	Triglycerides in large HDL	mmol/L
M-HDL-P	Concentration of medium HDL particles	mol/L
M-HDL-L	Total lipids in medium HDL	mmol/L
M-HDL-PL	Phospholipids in medium HDL	mmol/L
M-HDL-C	Total cholesterol in medium HDL	mmol/L
M-HDL-CE	Cholesterol esters in medium HDL	mmol/L
M-HDL-FC	Free cholesterol in medium HDL	mmol/L
M-HDL-TG	Triglycerides in medium HDL	mmol/L
S-HDL-P	Concentration of small HDL particles	mol/L
S-HDL-L	Total lipids in small HDL	mmol/L
S-HDL-PL	Phospholipids in small HDL	mmol/L
S-HDL-C	Total cholesterol in small HDL	mmol/L
S-HDL-CE	Cholesterol esters in small HDL	mmol/L
S-HDL-FC	Free cholesterol in small HDL	mmol/L
S-HDL-TG	Triglycerides in small HDL	mmol/L
XL-HDL-PL_%	Phospholipids to total lipids ratio in very large HDL	%
XL-HDL-C_%	Total cholesterol to total lipids ratio in very large HDL	%
XL-HDL-CE_%	Cholesterol esters to total lipids ratio in very large HDL	%
XL-HDL-FC_%	Free cholesterol to total lipids ratio in very large HDL	%
XL-HDL-TG_%	Triglycerides to total lipids ratio in very large HDL	%
L-HDL-PL_%	Phospholipids to total lipids ratio in large HDL	%
L-HDL-C_%	Total cholesterol to total lipids ratio in large HDL	%
L-HDL-CE_%	Cholesterol esters to total lipids ratio in large HDL	%
L-HDL-FC_%	Free cholesterol to total lipids ratio in large HDL	%
L-HDL-TG_%	Triglycerides to total lipids ratio in large HDL	%
M-HDL-PL_%	Phospholipids to total lipids ratio in medium HDL	%
M-HDL-C_%	Total cholesterol to total lipids ratio in medium HDL	%
M-HDL-CE_%	Cholesterol esters to total lipids ratio in medium HDL	%
M-HDL-FC_%	Free cholesterol to total lipids ratio in medium HDL	%
M-HDL-TG_%	Triglycerides to total lipids ratio in medium HDL	%
S-HDL-PL_%	Phospholipids to total lipids ratio in small HDL	%

S-HDL-C_%	Total cholesterol to total lipids ratio in small HDL	%
S-HDL-CE_%	Cholesterol esters to total lipids ratio in small HDL	%
S-HDL-FC_%	Free cholesterol to total lipids ratio in small HDL	%
S-HDL-TG_%	Triglycerides to total lipids ratio in small HDL	%
HDL-D	Mean diameter for HDL particles	nm
HDL-C	Total cholesterol in HDL	mmol/L
HDL2-C	Total cholesterol in HDL2	mmol/L
HDL3-C	Total cholesterol in HDL3	mmol/L
HDL-TG	Triglycerides in HDL	mmol/L

IDL-P	Concentration of IDL particles	mol/L
IDL-L	Total lipids in IDL	mmol/L
IDL-PL	Phospholipids in IDL	mmol/L
IDL-C	Total cholesterol in IDL	mmol/L
IDL-CE	Cholesterol esters in IDL	mmol/L
IDL-FC	Free cholesterol in IDL	mmol/L
IDL-TG	Triglycerides in IDL	mmol/L
IDL-PL_%	Phospholipids to total lipids ratio in IDL	%
IDL-C_%	Total cholesterol to total lipids ratio in IDL	%
IDL-CE_%	Cholesterol esters to total lipids ratio in IDL	%
IDL-FC_%	Free cholesterol to total lipids ratio in IDL	%
IDL-TG_%	Triglycerides to total lipids ratio in IDL	%

L-LDL-P	Concentration of large LDL particles	mol/L
L-LDL-L	Total lipids in large LDL	mmol/L
L-LDL-PL	Phospholipids in large LDL	mmol/L
L-LDL-C	Total cholesterol in large LDL	mmol/L
L-LDL-CE	Cholesterol esters in large LDL	mmol/L
L-LDL-FC	Free cholesterol in large LDL	mmol/L
L-LDL-TG	Triglycerides in large LDL	mmol/L
M-LDL-P	Concentration of medium LDL particles	mol/L
M-LDL-L	Total lipids in medium LDL	mmol/L
M-LDL-PL	Phospholipids in medium LDL	mmol/L
M-LDL-C	Total cholesterol in medium LDL	mmol/L
M-LDL-CE	Cholesterol esters in medium LDL	mmol/L
M-LDL-FC	Free cholesterol in medium LDL	mmol/L
M-LDL-TG	Triglycerides in medium LDL	mmol/L
S-LDL-P	Concentration of small LDL particles	mol/L
S-LDL-L	Total lipids in small LDL	mmol/L
S-LDL-PL	Phospholipids in small LDL	mmol/L
S-LDL-C	Total cholesterol in small LDL	mmol/L
S-LDL-CE	Cholesterol esters in small LDL	mmol/L
S-LDL-FC	Free cholesterol in small LDL	mmol/L
S-LDL-TG	Triglycerides in small LDL	mmol/L

L-LDL-PL_%	Phospholipids to total lipids ratio in large LDL	%
L-LDL-C_%	Total cholesterol to total lipids ratio in large LDL	%
L-LDL-CE_%	Cholesterol esters to total lipids ratio in large LDL	%
L-LDL-FC_%	Free cholesterol to total lipids ratio in large LDL	%
L-LDL-TG_%	Triglycerides to total lipids ratio in large LDL	%
M-LDL-PL_%	Phospholipids to total lipids ratio in medium LDL	%
M-LDL-C_%	Total cholesterol to total lipids ratio in medium LDL	%
M-LDL-CE_%	Cholesterol esters to total lipids ratio in medium LDL	%
M-LDL-FC_%	Free cholesterol to total lipids ratio in medium LDL	%
M-LDL-TG_%	Triglycerides to total lipids ratio in medium LDL	%
S-LDL-PL_%	Phospholipids to total lipids ratio in small LDL	%
S-LDL-C_%	Total cholesterol to total lipids ratio in small LDL	%
S-LDL-CE_%	Cholesterol esters to total lipids ratio in small LDL	%
S-LDL-FC_%	Free cholesterol to total lipids ratio in small LDL	%
S-LDL-TG_%	Triglycerides to total lipids ratio in small LDL	%
LDL-D	Mean diameter for LDL particles	nm
LDL-C	Total cholesterol in LDL	mmol/L
LDL-TG	Triglycerides in LDL	mmol/L
XXL-VLDL-P	Concentration of chylomicrons and extremely large VLDL particles	mol/L
XXL-VLDL-L	Total lipids in chylomicrons and extremely large VLDL particles	mmol/L
XXL-VLDL-PL	Phospholipids in chylomicrons and extremely large VLDL particles	mmol/L
XXL-VLDL-C	Total cholesterol in chylomicrons and extremely large VLDL particles	mmol/L
XXL-VLDL-CE	Cholesterol esters in chylomicrons and extremely large VLDL particles	mmol/L
XXL-VLDL-FC	Free cholesterol in chylomicrons and extremely large VLDL particles	mmol/L
XXL-VLDL-TG	Triglycerides in chylomicrons and extremely large VLDL particles	mmol/L
XL-VLDL-P	Concentration of very large VLDL particles	mol/L
XL-VLDL-L	Total lipids in very large VLDL	mmol/L
XL-VLDL-PL	Phospholipids in very large VLDL	mmol/L
XL-VLDL-C	Total cholesterol in very large VLDL	mmol/L
XL-VLDL-CE	Cholesterol esters in very large VLDL	mmol/L
XL-VLDL-FC	Free cholesterol in very large VLDL	mmol/L
XL-VLDL-TG	Triglycerides in very large VLDL	mmol/L
L-VLDL-P	Concentration of large VLDL particles	mol/L
L-VLDL-L	Total lipids in large VLDL	mmol/L
L-VLDL-PL	Phospholipids in large VLDL	mmol/L
L-VLDL-C	Total cholesterol in large VLDL	mmol/L
L-VLDL-CE	Cholesterol esters in large VLDL	mmol/L
L-VLDL-FC	Free cholesterol in large VLDL	mmol/L

L-VLDL-TG	Triglycerides in large VLDL	mmol/L
M-VLDL-P	Concentration of medium VLDL particles	mol/L
M-VLDL-L	Total lipids in medium VLDL	mmol/L
M-VLDL-PL	Phospholipids in medium VLDL	mmol/L
M-VLDL-C	Total cholesterol in medium VLDL	mmol/L
M-VLDL-CE	Cholesterol esters in medium VLDL	mmol/L
M-VLDL-FC	Free cholesterol in medium VLDL	mmol/L
M-VLDL-TG	Triglycerides in medium VLDL	mmol/L
S-VLDL-P	Concentration of small VLDL particles	mol/L
S-VLDL-L	Total lipids in small VLDL	mmol/L
S-VLDL-PL	Phospholipids in small VLDL	mmol/L
S-VLDL-C	Total cholesterol in small VLDL	mmol/L
S-VLDL-CE	Cholesterol esters in small VLDL	mmol/L
S-VLDL-FC	Free cholesterol in small VLDL	mmol/L
S-VLDL-TG	Triglycerides in small VLDL	mmol/L
XS-VLDL-P	Concentration of very small VLDL particles	mol/L
XS-VLDL-L	Total lipids in very small VLDL	mmol/L
XS-VLDL-PL	Phospholipids in very small VLDL	mmol/L
XS-VLDL-C	Total cholesterol in very small VLDL	mmol/L
XS-VLDL-CE	Cholesterol esters in very small VLDL	mmol/L
XS-VLDL-FC	Free cholesterol in very small VLDL	mmol/L
XS-VLDL-TG	Triglycerides in very small VLDL	mmol/L
XXL-VLDL-PL_%	Phospholipids to total lipids ratio in chylomicrons and extremely large VLDL	%
XXL-VLDL-C_%	Total cholesterol to total lipids ratio in chylomicrons and extremely large VLDL	%
XXL-VLDL-CE_%	Cholesterol esters to total lipids ratio in chylomicrons and extremely large VLDL	%
XXL-VLDL-FC_%	Free cholesterol to total lipids ratio in chylomicrons and extremely large VLDL	%
XXL-VLDL-TG_%	Triglycerides to total lipids ratio in chylomicrons and extremely large VLDL	%
XL-VLDL-PL_%	Phospholipids to total lipids ratio in very large VLDL	%
XL-VLDL-C_%	Total cholesterol to total lipids ratio in very large VLDL	%
XL-VLDL-CE_%	Cholesterol esters to total lipids ratio in very large VLDL	%
XL-VLDL-FC_%	Free cholesterol to total lipids ratio in very large VLDL	%
XL-VLDL-TG_%	Triglycerides to total lipids ratio in very large VLDL	%
L-VLDL-PL_%	Phospholipids to total lipids ratio in large VLDL	%
L-VLDL-C_%	Total cholesterol to total lipids ratio in large VLDL	%
L-VLDL-CE_%	Cholesterol esters to total lipids ratio in large VLDL	%
L-VLDL-FC_%	Free cholesterol to total lipids ratio in large VLDL	%
L-VLDL-TG_%	Triglycerides to total lipids ratio in large VLDL	%
M-VLDL-PL_%	Phospholipids to total lipids ratio in medium VLDL	%
M-VLDL-C_%	Total cholesterol to total lipids ratio in medium VLDL	%
M-VLDL-CE_%	Cholesterol esters to total lipids ratio in medium VLDL	%
M-VLDL-FC_%	Free cholesterol to total lipids ratio in medium VLDL	%

M-VLDL-TG_%	Triglycerides to total lipids ratio in medium VLDL	%
S-VLDL-PL_%	Phospholipids to total lipids ratio in small VLDL	%
S-VLDL-C_%	Total cholesterol to total lipids ratio in small VLDL	%
S-VLDL-CE_%	Cholesterol esters to total lipids ratio in small VLDL	%
S-VLDL-FC_%	Free cholesterol to total lipids ratio in small VLDL	%
S-VLDL-TG_%	Triglycerides to total lipids ratio in small VLDL	%
XS-VLDL-PL_%	Phospholipids to total lipids ratio in very small VLDL	%
XS-VLDL-C_%	Total cholesterol to total lipids ratio in very small VLDL	%
XS-VLDL-CE_%	Cholesterol esters to total lipids ratio in very small VLDL	%
XS-VLDL-FC_%	Free cholesterol to total lipids ratio in very small VLDL	%
XS-VLDL-TG_%	Triglycerides to total lipids ratio in very small VLDL	%
VLDL-D	Mean diameter for VLDL particles	nm
VLDL-C	Total cholesterol in VLDL	mmol/L
VLDL-TG	Triglycerides in VLDL	mmol/L
ApoA1	Apolipoprotein A-1	g/L
ApoB	Apolipoprotein B	g/L
ApoB/ApoA1	Ratio of apolipoprotein B to apolipoprotein A-1	
Serum-C	Serum total cholesterol	mmol/L
EstC	Esterified cholesterol	mmol/L
FreeC	Free cholesterol	mmol/L
Remnant-C	Remnant cholesterol (non-HDL, non-LDL cholesterol)	mmol/L
Serum-TG	Serum total triglycerides	mmol/L
TotPG	Total phosphoglycerides	mmol/L
TG/PG	Ratio of triglycerides to phosphoglycerides	
PC	Phosphatidylcholine and other cholines	mmol/L
SM	Sphingomyelins	mmol/L
TotCho	Total cholines	mmol/L
TotFA	Total fatty acids	mmol/L
UnsatDeg	Estimated degree of unsaturation	
DHA	22:6, docosahexaenoic acid	mmol/L
LA	18:2, linoleic acid	mmol/L
FAw3	Omega-3 fatty acids	mmol/L
FAw6	Omega-6 fatty acids	mmol/L
PUFA	Polyunsaturated fatty acids	mmol/L
MUFA	Monounsaturated fatty acids, mainly 16:1 and 18:1	mmol/L
SFA	Saturated fatty acids	mmol/L
DHA/FA	Ratio of 22:6 docosahexaenoic acid to total fatty acids	%
LA/FA	Ratio of 18:2 linoleic acid to total fatty acids	%
FAw3/FA	Ratio of omega-3 fatty acids to total fatty acids	%
FAw6/FA	Ratio of omega-6 fatty acids to total fatty acids	%
PUFA/FA	Ratio of polyunsaturated fatty acids to total fatty acids	%
MUFA/FA	Ratio of monounsaturated fatty acids to total fatty acids	%
SFA/FA	Ratio of saturated fatty acids to total fatty acids	%
Glc	Glucose	mmol/L

Lac	Lactate	mmol/L
Cit	Citrate	mmol/L
Ala	Alanine	mmol/L
Gln	Glutamine	mmol/L
His	Histidine	mmol/L
Ile	Isoleucine	mmol/L
Leu	Leucine	mmol/L
Val	Valine	mmol/L
Phe	Phenylalanine	mmol/L
Tyr	Tyrosine	mmol/L
Ace	Acetate	mmol/L
bOHBut	3-hydroxybutyrate	mmol/L
Crea	Creatinine	mmol/L
Alb	Albumin	signal area
Gp	Glycoprotein acetyls, mainly a1-acid glycoprotein	mmol/L

Table of NEO metabolites with median (IQR) concentration values, percent missing, and coefficient of variation

Metabolite	Measured	Missing	Median	25 percentile	75th percentile	Percentage missing	CV % (within-subject)	Unit
XXLVLDLP	2058	478	1.06E-10	6.67E-11	1.65E-10	25.151	12.294	mol/L
XXLVLDLL	2058	478	2.23E-02	1.39E-02	3.51E-02	25.151	12.295	mmol/L
XXLVLDLPL	2058	478	2.61E-03	1.55E-03	4.21E-03	25.151	12.303	mmol/L
XXLVLDLC	2058	478	3.22E-03	1.59E-03	5.62E-03	25.151	12.358	mmol/L
XXLVLDLCE	2058	478	1.68E-03	7.89E-04	3.10E-03	25.151	12.779	mmol/L
XXLVLDLFC	2058	478	1.53E-03	8.25E-04	2.59E-03	25.151	12.327	mmol/L
XXLVLDLTG	2058	478	1.66E-02	1.06E-02	2.53E-02	25.151	12.294	mmol/L
XLVLDLP	2183	353	5.81E-10	3.35E-10	9.58E-10	20.135	12.292	mol/L
XLVLDLL	2183	353	5.55E-02	3.13E-02	9.21E-02	20.135	12.292	mmol/L
XLVLDLPL	2183	353	8.43E-03	4.48E-03	1.46E-02	20.135	12.327	mmol/L
XLVLDLC	2183	353	9.13E-03	4.23E-03	1.61E-02	20.135	12.338	mmol/L
XLVLDLCE	2183	353	5.11E-03	2.54E-03	9.04E-03	20.135	12.344	mmol/L
XLVLDLFC	2183	353	3.95E-03	1.64E-03	7.17E-03	20.135	12.641	mmol/L
XLVLDLTG	2183	353	3.77E-02	2.27E-02	6.20E-02	20.135	12.293	mmol/L
LVLDLP	2439	97	4.13E-09	2.53E-09	6.45E-09	6.401	8.690	mol/L
LVLDLL	2439	97	2.34E-01	1.42E-01	3.70E-01	6.401	8.690	mmol/L
LVLDLPL	2439	97	4.25E-02	2.58E-02	6.66E-02	6.401	8.694	mmol/L
LVLDLC	2439	97	4.56E-02	2.47E-02	7.60E-02	6.401	8.694	mmol/L
LVLDLCE	2439	97	2.50E-02	1.45E-02	4.01E-02	6.401	8.697	mmol/L
LVLDLFC	2439	97	2.06E-02	1.02E-02	3.58E-02	6.401	8.723	mmol/L
LVLDLTG	2439	97	1.46E-01	9.10E-02	2.26E-01	6.401	8.692	mmol/L
MVLDLP	2531	5	1.48E-08	1.02E-08	2.11E-08	0.260	0.129	mol/L
MVLDLL	2531	5	4.92E-01	3.36E-01	6.95E-01	0.260	0.114	mmol/L
MVLDLPL	2531	5	9.99E-02	6.98E-02	1.39E-01	0.260	0.230	mmol/L
MVLDLC	2531	5	1.20E-01	8.07E-02	1.73E-01	0.260	0.165	mmol/L
MVLDLCE	2531	5	6.73E-02	4.67E-02	9.46E-02	0.260	0.287	mmol/L
MVLDLFC	2531	5	5.38E-02	3.47E-02	7.89E-02	0.260	0.322	mmol/L
MVLDLTG	2531	5	2.71E-01	1.86E-01	3.87E-01	0.260	0.202	mmol/L
SVLDLP	2529	7	2.62E-08	2.04E-08	3.27E-08	0.271	0.072	mol/L
SVLDLL	2529	7	5.05E-01	3.93E-01	6.35E-01	0.271	0.070	mmol/L
SVLDLPL	2529	7	1.25E-01	1.02E-01	1.52E-01	0.271	0.098	mmol/L
SVLDLC	2529	7	1.61E-01	1.22E-01	2.07E-01	0.271	0.141	mmol/L
SVLDLCE	2529	7	9.15E-02	6.51E-02	1.21E-01	0.271	0.217	mmol/L

SVLDLFC	2529	7	6.99E-02	5.53E-02	8.69E-02	0.271	0.096	mmol/L
SVLDLTG	2529	7	2.18E-01	1.70E-01	2.83E-01	0.271	0.123	mmol/L
XSVLDLP	2533	3	3.21E-08	2.67E-08	3.73E-08	0.111	0.086	mol/L
XSVLDLL	2533	3	4.01E-01	3.33E-01	4.66E-01	0.111	0.094	mmol/L
XSVLDLPL	2533	3	1.31E-01	1.10E-01	1.53E-01	0.111	0.052	mmol/L
XSVLDLC	2533	3	1.74E-01	1.38E-01	2.08E-01	0.111	0.185	mmol/L
XSVLDLCE	2533	3	1.11E-01	8.61E-02	1.35E-01	0.111	0.250	mmol/L
XSVLDLFC	2533	3	6.25E-02	5.13E-02	7.32E-02	0.111	0.078	mmol/L
XSVLDLTG	2533	3	9.47E-02	7.96E-02	1.15E-01	0.111	0.099	mmol/L
IDLP	2536	0	9.20E-08	7.76E-08	1.08E-07	0.000	0.053	mol/L
IDLL	2536	0	9.32E-01	7.79E-01	1.09E+00	0.000	0.056	mmol/L
IDLPL	2533	3	2.62E-01	2.23E-01	3.03E-01	0.040	0.047	mmol/L
IDLC	2533	3	5.72E-01	4.64E-01	6.88E-01	0.040	0.071	mmol/L
IDLCE	2533	3	4.01E-01	3.24E-01	4.82E-01	0.040	0.083	mmol/L
IDLFC	2533	3	1.71E-01	1.41E-01	2.03E-01	0.040	0.058	mmol/L
IDLTG	2533	3	9.86E-02	8.63E-02	1.13E-01	0.040	0.083	mmol/L
LLDLP	2535	1	1.60E-07	1.34E-07	1.88E-07	0.013	0.032	mol/L
LLDLL	2535	1	1.14E+00	9.55E-01	1.34E+00	0.013	0.033	mmol/L
LLDLPL	2535	1	2.91E-01	2.53E-01	3.34E-01	0.013	0.031	mmol/L
LLDLC	2535	1	7.62E-01	6.27E-01	9.12E-01	0.013	0.036	mmol/L
LLDLCE	2535	1	5.42E-01	4.42E-01	6.61E-01	0.013	0.039	mmol/L
LLDLFC	2535	1	2.19E-01	1.85E-01	2.57E-01	0.013	0.046	mmol/L
LLDLTG	2535	1	8.47E-02	7.26E-02	9.77E-02	0.013	0.089	mmol/L
MLDLP	2534	2	1.32E-07	1.11E-07	1.57E-07	0.026	0.027	mol/L
MLDLL	2534	2	6.69E-01	5.63E-01	7.95E-01	0.026	0.018	mmol/L
MLDLPL	2534	2	1.82E-01	1.59E-01	2.07E-01	0.026	0.032	mmol/L
MLDLC	2534	2	4.47E-01	3.63E-01	5.42E-01	0.026	0.026	mmol/L
MLDLCE	2534	2	3.22E-01	2.54E-01	3.99E-01	0.026	0.117	mmol/L
MLDLFC	2534	2	1.25E-01	1.09E-01	1.43E-01	0.026	0.037	mmol/L
MLDLTG	2534	2	4.37E-02	3.70E-02	5.07E-02	0.026	0.137	mmol/L
SLDLP	2534	2	1.54E-07	1.29E-07	1.82E-07	0.026	0.027	mol/L
SLDLL	2534	2	4.30E-01	3.62E-01	5.09E-01	0.026	0.020	mmol/L
SLDLPL	2534	2	1.32E-01	1.16E-01	1.49E-01	0.026	0.034	mmol/L
SLDLC	2534	2	2.71E-01	2.19E-01	3.30E-01	0.026	0.028	mmol/L
SLDLCE	2534	2	1.98E-01	1.55E-01	2.44E-01	0.026	0.043	mmol/L
SLDLFC	2534	2	7.38E-02	6.36E-02	8.45E-02	0.026	0.031	mmol/L

SLDLTG	2534	2	2.74E-02	2.32E-02	3.25E-02	0.026	0.140	mmol/L
XLHDLP	2419	117	3.51E-07	2.43E-07	4.90E-07	3.494	8.689	mol/L
XLHDLL	2419	117	3.51E-01	2.42E-01	4.93E-01	3.494	8.689	mmol/L
XLHDLPL	2419	117	1.85E-01	1.18E-01	2.69E-01	3.494	8.691	mmol/L
XLHDLC	2419	117	1.53E-01	1.11E-01	2.13E-01	3.494	8.691	mmol/L
XLHDLCE	2419	117	1.13E-01	8.39E-02	1.55E-01	3.494	8.691	mmol/L
XLHDLFC	2419	117	4.05E-02	2.61E-02	5.84E-02	3.494	8.698	mmol/L
XLHDLTG	2419	117	1.22E-02	8.44E-03	1.59E-02	3.494	8.693	mmol/L
LHDLP	2406	130	1.12E-06	8.02E-07	1.51E-06	3.622	0.093	mol/L
LHDLL	2406	130	7.02E-01	4.99E-01	9.52E-01	3.622	0.091	mmol/L
LHDLPL	2406	130	3.58E-01	2.67E-01	4.67E-01	3.622	0.129	mmol/L
LHDLC	2406	130	3.22E-01	2.12E-01	4.53E-01	3.622	0.137	mmol/L
LHDLCE	2406	130	2.49E-01	1.67E-01	3.49E-01	3.622	0.142	mmol/L
LHDLFC	2406	130	7.12E-02	4.51E-02	1.04E-01	3.622	0.510	mmol/L
LHDLTG	2406	130	2.45E-02	1.88E-02	3.26E-02	3.622	0.347	mmol/L
MHDLP	2524	12	2.14E-06	1.90E-06	2.38E-06	0.400	0.046	mol/L
MHDLL	2524	12	9.07E-01	8.02E-01	1.01E+00	0.400	0.049	mmol/L
MHDLPL	2524	12	4.19E-01	3.72E-01	4.69E-01	0.400	0.041	mmol/L
MHDLC	2524	12	4.43E-01	3.82E-01	5.00E-01	0.400	0.061	mmol/L
MHDLCE	2524	12	3.60E-01	3.13E-01	4.07E-01	0.400	0.063	mmol/L
MHDLFC	2524	12	8.22E-02	6.92E-02	9.47E-02	0.400	0.078	mmol/L
MHDLTG	2524	12	4.62E-02	4.02E-02	5.33E-02	0.400	0.087	mmol/L
SHDLP	2531	5	4.95E-06	4.69E-06	5.25E-06	0.074	0.036	mol/L
SHDLL	2531	5	1.10E+00	1.04E+00	1.16E+00	0.074	0.041	mmol/L
SHDLPL	2531	5	5.95E-01	5.58E-01	6.34E-01	0.074	0.026	mmol/L
SHDLC	2531	5	4.51E-01	4.17E-01	4.87E-01	0.074	0.059	mmol/L
SHDLCE	2531	5	3.44E-01	3.12E-01	3.76E-01	0.074	0.072	mmol/L
SHDLFC	2531	5	1.08E-01	1.01E-01	1.14E-01	0.074	0.034	mmol/L
SHDLTG	2531	5	5.02E-02	4.32E-02	5.86E-02	0.074	0.084	mmol/L
XXLVLDLPLp	2058	478	1.18E+01	1.09E+01	1.23E+01	25.151	0.451	%
XXLVLDLCp	2058	478	1.45E+01	1.18E+01	1.64E+01	25.151	1.093	%
XXLVLDLCEp	2058	478	7.88E+00	5.59E+00	9.29E+00	25.151	3.334	%
XXLVLDLFCp	2058	478	6.90E+00	5.65E+00	7.59E+00	25.151	0.830	%
XXLVLDLTGp	2058	478	7.39E+01	7.17E+01	7.72E+01	25.151	0.115	%
XLVLDLPLp	2183	353	1.54E+01	1.40E+01	1.61E+01	20.135	0.900	%
XLVLDLCp	2183	353	1.65E+01	1.36E+01	1.84E+01	20.135	0.952	%

XLVLDLCEp	2183	353	9.41E+00	7.88E+00	1.04E+01	20.135	1.027	%
XLVLDLFCp	2183	353	7.11E+00	5.42E+00	8.09E+00	20.135	2.886	%
XLVLDLTGp	2183	353	6.82E+01	6.56E+01	7.24E+01	20.135	0.230	%
LVLDLPLp	2439	97	1.82E+01	1.79E+01	1.86E+01	6.401	0.319	%
LVLDLCp	2439	97	1.96E+01	1.75E+01	2.10E+01	6.401	0.362	%
LVLDLCEp	2439	97	1.07E+01	9.80E+00	1.15E+01	6.401	0.399	%
LVLDLFCp	2439	97	8.88E+00	7.24E+00	9.84E+00	6.401	0.779	%
LVLDLTGp	2439	97	6.21E+01	6.07E+01	6.43E+01	6.401	0.139	%
MVLDLPLp	2531	5	2.04E+01	1.99E+01	2.09E+01	0.260	0.239	%
MVLDLCp	2531	5	2.46E+01	2.28E+01	2.62E+01	0.260	0.176	%
MVLDLCEp	2531	5	1.35E+01	1.19E+01	1.52E+01	0.260	0.286	%
MVLDLFCp	2531	5	1.10E+01	1.05E+01	1.14E+01	0.260	0.333	%
MVLDLTGp	2531	5	5.52E+01	5.32E+01	5.70E+01	0.260	0.123	%
SVLDLPLp	2529	7	2.45E+01	2.33E+01	2.61E+01	0.271	0.086	%
SVLDLCp	2529	7	3.17E+01	2.86E+01	3.42E+01	0.271	0.110	%
SVLDLCEp	2529	7	1.79E+01	1.48E+01	2.04E+01	0.271	0.186	%
SVLDLFCp	2529	7	1.37E+01	1.34E+01	1.41E+01	0.271	0.099	%
SVLDLTGp	2529	7	4.38E+01	4.13E+01	4.65E+01	0.271	0.105	%
XSVLDLPLp	2533	3	3.30E+01	3.13E+01	3.44E+01	0.111	0.069	%
XSVLDLCp	2533	3	4.32E+01	3.98E+01	4.57E+01	0.111	0.099	%
XSVLDLCEp	2533	3	2.75E+01	2.45E+01	2.99E+01	0.111	0.161	%
XSVLDLFCp	2533	3	1.56E+01	1.50E+01	1.61E+01	0.111	0.044	%
XSVLDLTGp	2533	3	2.38E+01	2.11E+01	2.78E+01	0.111	0.129	%
IDLPLp	2533	3	2.81E+01	2.75E+01	2.88E+01	0.040	0.033	%
IDLCp	2533	3	6.15E+01	5.90E+01	6.29E+01	0.040	0.024	%
IDLCEp	2533	3	4.32E+01	4.10E+01	4.45E+01	0.040	0.036	%
IDLFCp	2533	3	1.85E+01	1.78E+01	1.91E+01	0.040	0.037	%
IDLTGp	2533	3	1.05E+01	9.28E+00	1.25E+01	0.040	0.102	%
LLDLPLp	2535	1	2.56E+01	2.49E+01	2.65E+01	0.013	0.027	%
LLDLCp	2535	1	6.70E+01	6.53E+01	6.84E+01	0.013	0.015	%
LLDLCEp	2535	1	4.79E+01	4.58E+01	4.94E+01	0.013	0.022	%
LLDLFCp	2535	1	1.92E+01	1.87E+01	1.98E+01	0.013	0.035	%
LLDLTGp	2535	1	7.38E+00	6.51E+00	8.52E+00	0.013	0.088	%
MLDLPLp	2534	2	2.69E+01	2.57E+01	2.85E+01	0.026	0.029	%
MLDLCp	2534	2	6.67E+01	6.43E+01	6.85E+01	0.026	0.018	%
MLDLCEp	2534	2	4.80E+01	4.49E+01	5.04E+01	0.026	0.115	%

MLDLFCp	2534	2	1.86E+01	1.79E+01	1.95E+01	0.026	0.036	%
MLDLTGp	2534	2	6.39E+00	5.58E+00	7.48E+00	0.026	0.134	%
SLDLPLp	2534	2	3.05E+01	2.89E+01	3.24E+01	0.026	0.027	%
SLDLCp	2534	2	6.33E+01	6.05E+01	6.53E+01	0.026	0.018	%
SLDLCEp	2534	2	4.61E+01	4.28E+01	4.86E+01	0.026	0.029	%
SLDLFCp	2534	2	1.71E+01	1.65E+01	1.77E+01	0.026	0.038	%
SLDLTGp	2534	2	6.33E+00	5.53E+00	7.46E+00	0.026	0.131	%
XLHDLPLp	2419	117	5.31E+01	4.92E+01	5.55E+01	3.494	0.212	%
XLHDLCp	2419	117	4.38E+01	4.18E+01	4.65E+01	3.494	0.141	%
XLHDLCEp	2419	117	3.22E+01	3.02E+01	3.54E+01	3.494	0.141	%
XLHDLFCp	2419	117	1.16E+01	1.08E+01	1.22E+01	3.494	0.339	%
XLHDLTGp	2419	117	3.05E+00	2.33E+00	4.53E+00	3.494	0.241	%
LHDLPLp	2406	130	5.09E+01	4.87E+01	5.35E+01	3.622	0.084	%
LHDLCp	2406	130	4.58E+01	4.25E+01	4.80E+01	3.622	0.112	%
LHDLCEp	2406	130	3.56E+01	3.35E+01	3.71E+01	3.622	0.127	%
LHDLFCp	2406	130	1.02E+01	9.03E+00	1.09E+01	3.622	0.484	%
LHDLTGp	2406	130	3.46E+00	3.02E+00	4.09E+00	3.622	0.317	%
MHDLPLp	2524	12	4.63E+01	4.57E+01	4.70E+01	0.400	0.023	%
MHDLCp	2524	12	4.87E+01	4.71E+01	4.98E+01	0.400	0.024	%
MHDLCEp	2524	12	3.96E+01	3.83E+01	4.06E+01	0.400	0.027	%
MHDLFCp	2524	12	9.08E+00	8.64E+00	9.41E+00	0.400	0.058	%
MHDLTGp	2524	12	5.01E+00	4.29E+00	6.03E+00	0.400	0.099	%
SHDLPLp	2531	5	5.43E+01	5.26E+01	5.59E+01	0.074	0.019	%
SHDLCp	2531	5	4.12E+01	3.94E+01	4.29E+01	0.074	0.028	%
SHDLCEp	2531	5	3.13E+01	2.94E+01	3.33E+01	0.074	0.040	%
SHDLFCp	2531	5	9.81E+00	9.56E+00	1.01E+01	0.074	0.026	%
SHDLTGp	2531	5	4.51E+00	3.96E+00	5.28E+00	0.074	0.088	%
VLDLD	2536	0	3.71E+01	3.62E+01	3.79E+01	0.000	0.011	nm
LDLD	2536	0	2.35E+01	2.34E+01	2.35E+01	0.000	0.006	nm
HDLD	2536	0	9.90E+00	9.74E+00	1.01E+01	0.000	0.007	nm
SerumC	2536	0	4.00E+00	3.48E+00	4.58E+00	0.000	0.027	mmol/L
VLDLC	2536	0	5.10E-01	3.80E-01	6.81E-01	0.000	0.156	mmol/L
RemnantC	2536	0	1.10E+00	8.69E-01	1.33E+00	0.000	0.105	mmol/L
LDLC	2536	0	1.48E+00	1.21E+00	1.78E+00	0.000	0.027	mmol/L
HDLC	2536	0	1.37E+00	1.15E+00	1.62E+00	0.000	0.047	mmol/L
HDL2C	2530	6	9.16E-01	7.12E-01	1.15E+00	0.087	0.104	mmol/L

HDL3C	2536	0	4.58E-01	4.41E-01	4.79E-01	0.000	0.164	mmol/L
EstC	2525	11	2.80E+00	2.43E+00	3.23E+00	1.069	0.620	mmol/L
FreeC	2532	4	1.20E+00	1.04E+00	1.36E+00	0.466	1.411	mmol/L
SerumTG	2536	0	1.15E+00	9.01E-01	1.50E+00	0.000	0.086	mmol/L
VLDLTG	2536	0	7.62E-01	5.35E-01	1.07E+00	0.000	0.112	mmol/L
LDLTG	2536	0	1.56E-01	1.34E-01	1.81E-01	0.000	0.105	mmol/L
HDLTG	2536	0	1.35E-01	1.19E-01	1.51E-01	0.000	0.108	mmol/L
TotPG	2530	6	1.60E+00	1.38E+00	1.83E+00	0.622	0.853	mmol/L
TGPG	2495	41	5.31E-01	3.84E-01	7.35E-01	3.568	1.344	
PC	2432	104	1.71E+00	1.51E+00	1.96E+00	6.168	0.879	mmol/L
SM	2532	4	3.95E-01	3.46E-01	4.47E-01	0.466	0.837	mmol/L
TotCho	2533	3	1.96E+00	1.72E+00	2.22E+00	0.330	0.853	mmol/L
ApoA1	2536	0	1.47E+00	1.35E+00	1.61E+00	0.000	0.033	g/L
ApoB	2535	1	7.80E-01	6.60E-01	8.98E-01	0.017	0.056	g/L
ApoBApoA1	2535	1	5.25E-01	4.38E-01	6.27E-01	0.017	0.066	
TotFA	2527	9	9.56E+00	8.36E+00	1.09E+01	0.939	1.567	mmol/L
UnSat	2527	9	1.26E+00	1.21E+00	1.31E+00	0.939	1.158	
DHA	2524	12	1.11E-01	8.34E-02	1.42E-01	1.205	0.879	mmol/L
LA	2528	8	2.64E+00	2.27E+00	3.00E+00	0.906	1.278	mmol/L
FAw3	2530	6	3.53E-01	2.87E-01	4.34E-01	0.635	1.872	mmol/L
FAw6	2530	6	3.26E+00	2.84E+00	3.69E+00	0.635	1.203	mmol/L
PUFA	2528	8	3.64E+00	3.16E+00	4.10E+00	0.906	1.178	mmol/L
MUFA	2505	31	2.41E+00	2.06E+00	2.94E+00	2.528	0.892	mmol/L
SFA	2504	32	3.47E+00	2.98E+00	4.06E+00	2.541	3.446	mmol/L
DHAFA	2523	13	1.13E+00	9.18E-01	1.42E+00	1.237	1.225	%
LAFA	2527	9	2.76E+01	2.53E+01	2.98E+01	0.939	1.544	%
FAw3FA	2527	9	3.62E+00	3.17E+00	4.27E+00	0.939	2.003	%
FAw6FA	2527	9	3.42E+01	3.20E+01	3.62E+01	0.939	1.319	%
PUFAFA	2527	9	3.80E+01	3.57E+01	3.99E+01	0.939	1.305	%
MUFAFA	2503	33	2.57E+01	2.37E+01	2.80E+01	2.800	1.212	%
SFAFA	2502	34	3.65E+01	3.51E+01	3.78E+01	2.813	2.083	%
Glc	2535	1	4.17E+00	3.89E+00	4.50E+00	0.033	0.117	mmol/L
Lac	2536	0	1.04E+00	9.00E-01	1.23E+00	0.000	0.325	mmol/L
Cit	2536	0	1.50E-01	1.31E-01	1.69E-01	0.000	0.085	mmol/L
Ala	2536	0	3.43E-01	3.10E-01	3.84E-01	0.000	0.113	mmol/L
Gln	2536	0	4.76E-01	4.43E-01	5.09E-01	0.000	0.069	mmol/L

His	2536	0	5.48E-02	5.09E-02	5.90E-02	0.000	0.095	mmol/L
Ile	2535	1	4.76E-02	3.96E-02	5.75E-02	0.017	0.410	mmol/L
Leu	2535	1	6.46E-02	5.59E-02	7.45E-02	0.017	0.238	mmol/L
Val	2536	0	1.52E-01	1.35E-01	1.72E-01	0.000	0.159	mmol/L
Phe	2536	0	5.25E-02	4.90E-02	5.58E-02	0.000	0.120	mmol/L
Tyr	2536	0	5.25E-02	4.68E-02	5.86E-02	0.000	0.163	mmol/L
Ace	2536	0	4.47E-02	3.90E-02	5.31E-02	0.000	0.190	mmol/L
bOHBut	2532	4	1.18E-01	1.01E-01	1.41E-01	0.176	0.177	mmol/L
Crea	2536	0	6.33E-02	5.69E-02	7.03E-02	0.000	0.097	mmol/L
Alb	2536	0	8.57E-02	8.34E-02	8.83E-02	0.000	0.024	signal area
Gp	2535	1	1.19E+00	1.08E+00	1.31E+00	0.013	0.111	mmol/L

Table S2. Biochemical Pathways Identified from Metabolomics Analysis Associated with Visceral Adiposity.

Pathway Name	Total Pathway Metabolites	Metabolite Hits	Raw p-value	-log(p)	Impact
Aminoacyl-tRNA biosynthesis	75	9	3.39E-10	21.804	0.11268
Valine, leucine and isoleucine biosynthesis	27	4	2.71E-05	10.516	0.12825
Valine, leucine and isoleucine degradation	40	4	0.00013	8.9228	0.03889
Arginine and proline metabolism	77	5	0.00014	8.9125	0.2709
Alanine, aspartate and glutamate metabolism	24	3	0.00054	7.5224	0.44065
D-Glutamine and D-glutamate metabolism	11	2	0.00249	5.9962	0.13904
Galactose metabolism	41	3	0.00264	5.9355	0.00246
Pantothenate and CoA biosynthesis	27	2	0.01486	4.2092	0.07366
Glycolysis or Gluconeogenesis	31	2	0.01936	3.9445	0.01094
Amino sugar and nucleotide sugar metabolism	88	3	0.02215	3.8099	0.01122
Propanoate metabolism	35	2	0.02437	3.7145	0
Nitrogen metabolism	39	2	0.02985	3.5116	0
Fructose and mannose metabolism	48	2	0.04378	3.1285	0.03419
D-Arginine and D-ornithine metabolism	8	1	0.0552	2.8967	0
Biotin metabolism	11	1	0.07516	2.5882	0
Taurine and hypotaurine metabolism	20	1	0.13266	2.02	0.03237
Selenoamino acid metabolism	22	1	0.14497	1.9312	0
Glycerolipid metabolism	32	1	0.20411	1.5891	0.18847
Pyruvate metabolism	32	1	0.20411	1.5891	0.13756

Lysine biosynthesis	32	1	0.20411	1.5891	0.09993
Glutathione metabolism	38	1	0.23772	1.4367	0.01095
Glycerophospholipid metabolism	39	1	0.24319	1.4139	0.0212
Butanoate metabolism	40	1	0.24862	1.3918	0
Histidine metabolism	44	1	0.26999	1.3094	0.00051
Lysine degradation	47	1	0.28564	1.253	0.14675
Glycine, serine and threonine metabolism	48	1	0.29078	1.2352	0
Starch and sucrose metabolism	50	1	0.30097	1.2007	0.03116
Cysteine and methionine metabolism	56	1	0.33071	1.1065	0
Pyrimidine metabolism	60	1	0.34987	1.0502	0
Purine metabolism	92	1	0.48561	0.72235	0
Porphyrin and chlorophyll metabolism	104	1	0.52925	0.63629	0

Table S3. Spearman Correlation Coefficients for Body Mass Index, Visceral Adipose Tissue, and Selected Metabolites in MESA and NEO Studies.

	Visceral adipose tissue	Acetyl glyco-proteins	Lactate	Isoleucine	Leucine	Valine	Glutamine	HDL-cholesterol	Triglycerides	VLDL-cholesterol
Body mass index	0.60	0.22	0.21	0.24	0.13	0.17	-0.21	-0.23	0.25	0.08*
	0.55	0.35	0.22	0.28	0.26	0.27	-0.13	-0.22	0.25	0.18
Visceral adipose tissue		0.33	0.37	0.40	0.25	0.24	-0.24	-0.45	0.38	0.26
		0.43	0.33	0.54	0.54	0.45	-0.07*	-0.43	0.44	0.36
Acetylglycoproteins			0.86	0.74	0.59	0.39	-0.44	-0.54	0.79	0.74
			0.37	0.65	0.55	0.28	-0.07*	-0.43	0.81	0.70
Lactate				0.82	0.50	0.35	-0.51	-0.52	0.93	0.80
				0.43	0.39	0.29	-0.11	-0.24	0.38	0.30
Isoleucine					0.64	0.28	-0.48	-0.53	0.79	0.58
					0.92	0.72	0.04*	-0.60	0.76	0.65
Leucine						0.13	-0.30	-0.37	0.48	0.34
						0.83	0.05*	-0.50	0.64	0.55
Valine							-0.15	-0.28	0.28	0.23
							0.06*	-0.39	0.33	0.26
Glutamine								0.18	-0.59	-0.39
								-0.05*	-0.04*	-0.04*
HDL-cholesterol									-0.48	-0.48
									-0.56	-0.47
Triglycerides										0.77
										0.91

Top cell: MESA correlations
Bottom cell: NEO correlations
MESA: all P<0.0001 except *P=0.006
NEO: all P<0.0001 except *P<0.05 and **P=0.058

Figure S1. Metabolites Associated with Visceral Adiposity in Sex Stratified Analyses.

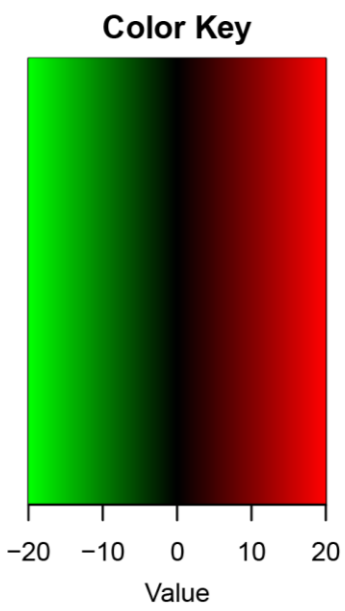

Beige = Lipids, Pink = CPMG, Blue = NOESY. # denotes statistical significance

Figure S2. Metabolites Associated with Visceral Adiposity in Race/Ethnicity Stratified Analyses.

MESA, sex-stratified

NEO, sex stratified

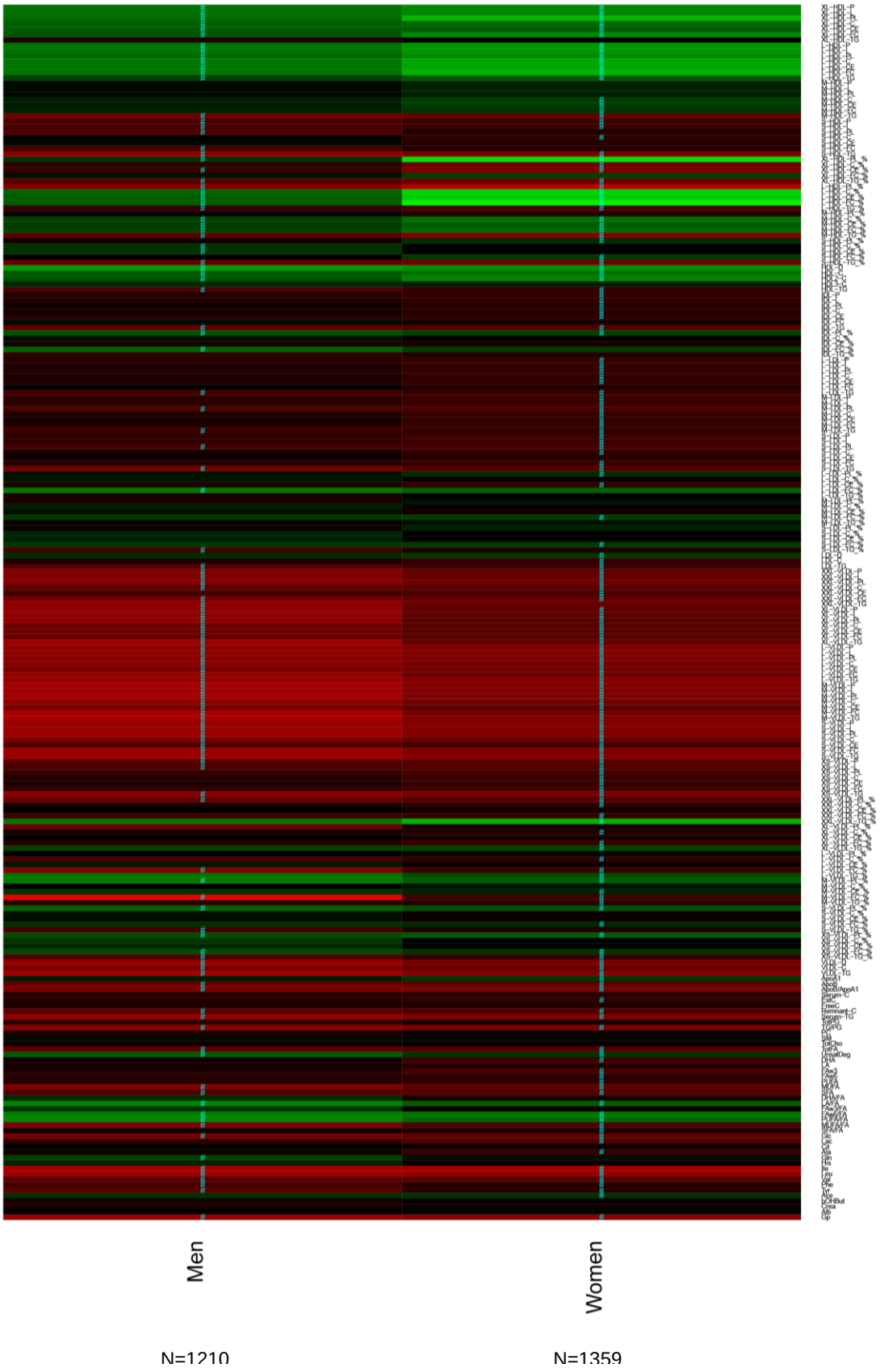

Beige = Lipids, Pink = CPMG, Blue = NOESY. # denotes statistical significance

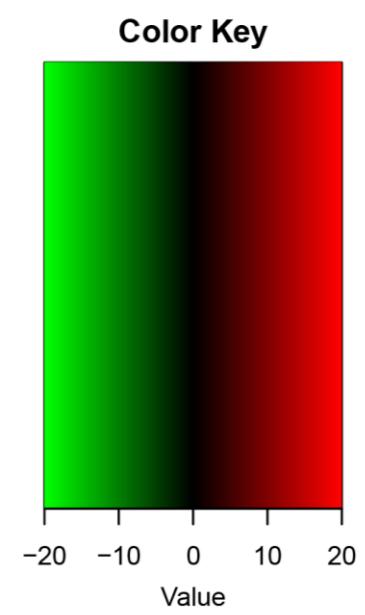

Figure S3. Mendelian Randomization Study of Genetic Traits Linked to Blood Lipid Levels with Visceral Adiposity.

MESA, race-stratified

NEO, race-stratified

N=439

N=664

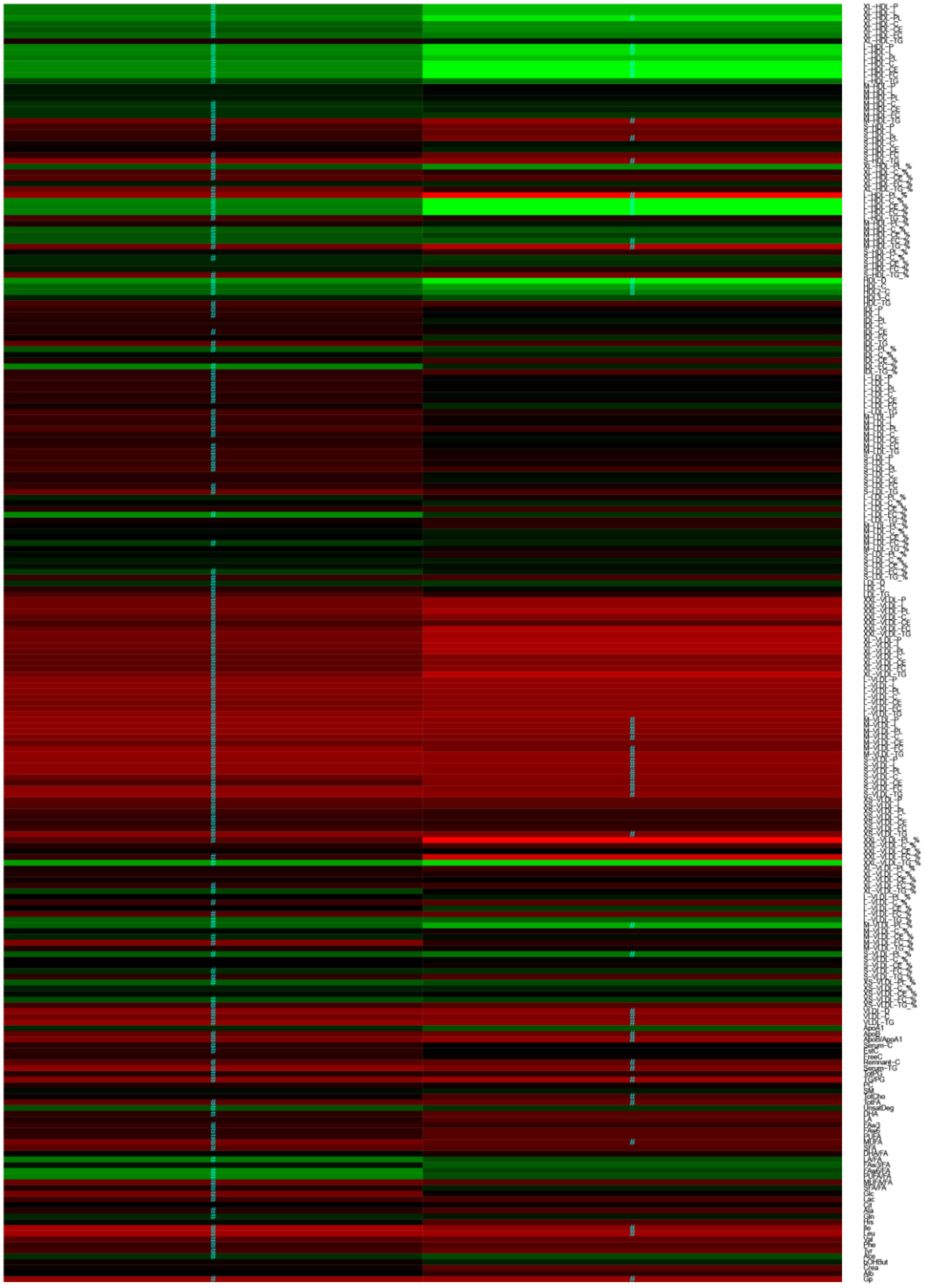

White

N=2456

Non–white

N=113

As shown in the tables below, the IVW estimators did not show statistical evidence of a causal effect of these lipid traits on VAT volume. Furthermore, the MR-Egger intercepts were not indicative of presence of directional pleiotropy, which is in line with the fairly symmetric funnel plots. Results from all sensitivity analyses were consistent with the corresponding IVW causal effect estimator, which further underscores the validity of these results.

We must however acknowledge several limitations of our analyses. These foremost include our use of summary statistics from a multiethnic GWAS meta-analysis, due to which we cannot fully exclude bias due to population stratification, and that the magnitude of our estimates are not interpretable. Finally, using genetic instruments for overall measures of blood lipid traits may not be representative for causal effects of the underlying lipoprotein subclasses.

High-density lipoprotein cholesterol (n=83 instruments)

Estimator	Beta	SE	p-value
Inverse Variance Weighted	-0.07	0.05	0.17
MR-Egger intercept	-0.002	0.004	0.59
MR-Egger slope	-0.03	0.10	0.78
Weighted median	-0.08	0.07	0.25
Weighted Mode-Based Estimator	-0.08	0.06	0.24

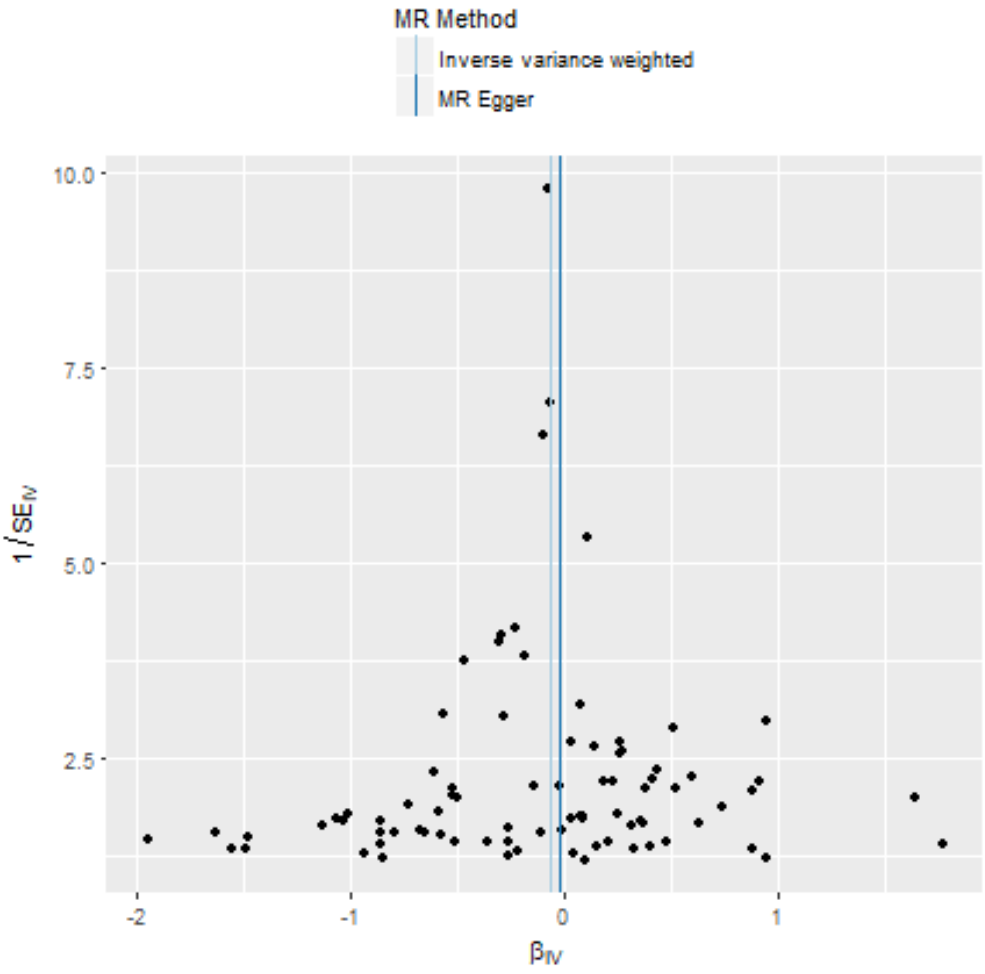

Low-density lipoprotein cholesterol (n=72 instruments)

Estimator	Beta	SE	p-value
Inverse Variance Weighted	-0.05	0.05	0.24
MR-Egger intercept	0.0004	0.004	0.92
MR-Egger slope	-0.06	0.07	0.42
Weighted median	-0.07	0.07	0.27

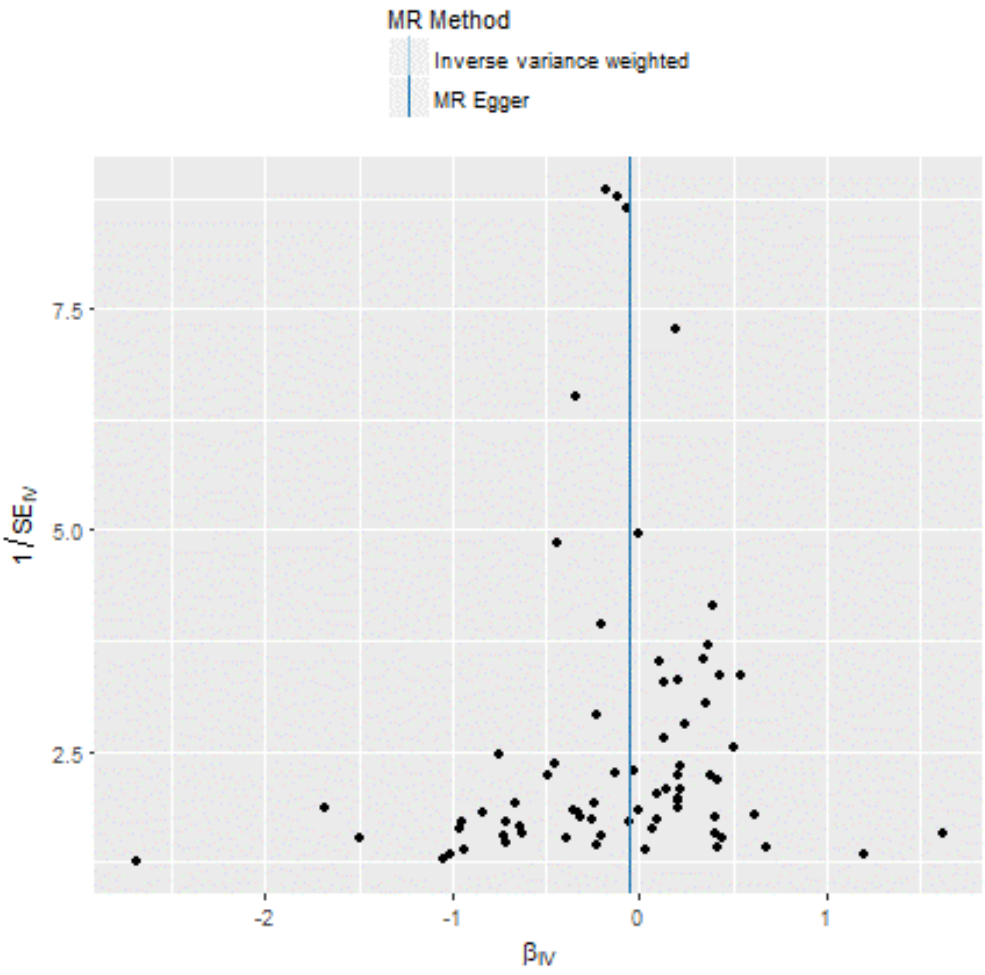

Triglycerides (n=53 instruments)

Estimator	Beta	SE	p-value
Inverse Variance Weighted	0.05	0.06	0.42
MR-Egger intercept	-0.004	0.005	0.45
MR-Egger slope	0.11	0.10	0.28
Weighted median	0.07	0.08	0.36
Weighted Mode-Based Estimator	0.11	0.07	0.14

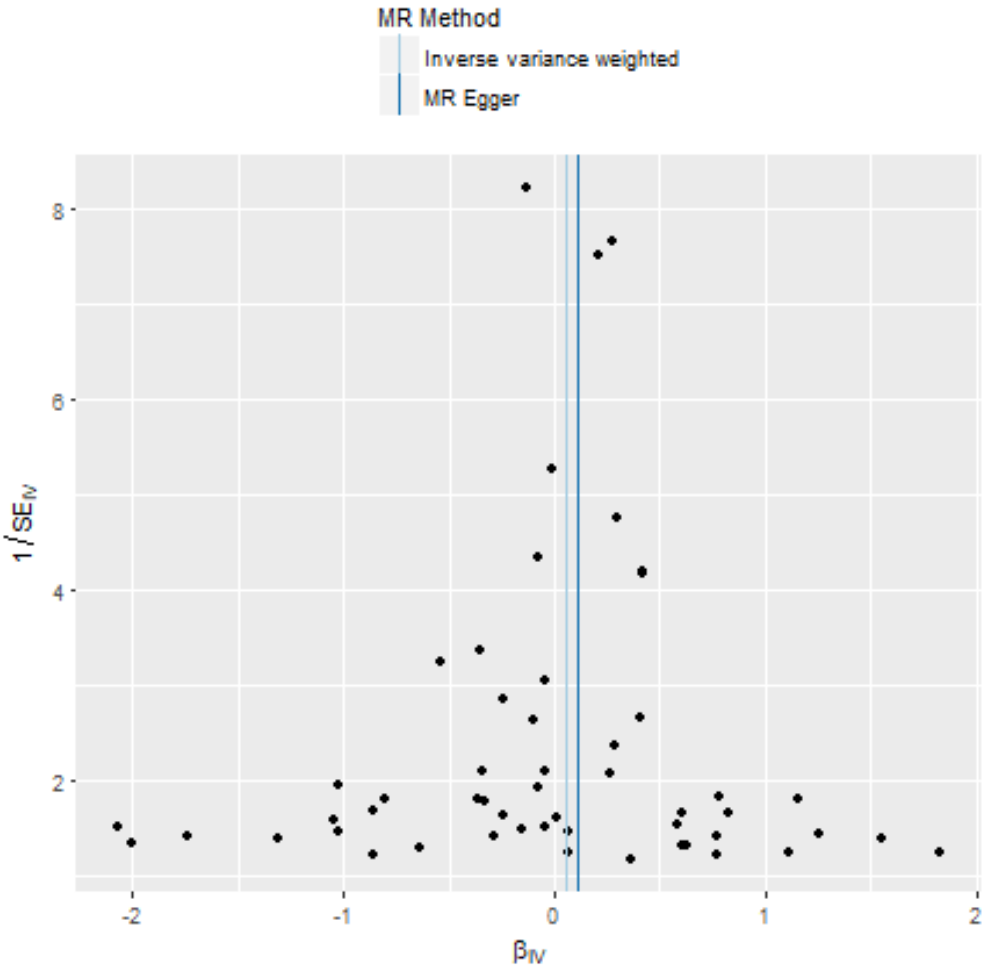

Supplemental References:

1. Chambers JC, Obeid OA, Refsum H, Ueland P, Hackett D, Hooper J, Turner RM, Thompson SG and Kooner JS. Plasma homocysteine concentrations and risk of coronary heart disease in UK Indian Asian and European men. *The Lancet*. 2000;355:523-527.

2. Hofman A, Murad S, van Duijn C, Franco O, Goedegebure A, Arfan Ikram M, Klaver CW, Nijsten TC, Peeters R, Stricker BC, Tiemeier H, Uitterlinden A and Vernooij M. The Rotterdam Study: 2014 objectives and design update. *Eur J Epidemiol*. 2013;28:889-926.

3. Dona AC, Jiménez B, Schäfer H, Humpfer E, Spraul M, Lewis MR, Pearce JTM, Holmes E, Lindon JC and Nicholson JK. Precision High-Throughput Proton NMR Spectroscopy of Human Urine, Serum, and Plasma for Large-Scale Metabolic Phenotyping. *Analytical Chemistry*. 2014;86:9887-9894.

4. Dona AC, Jimenez B, Schafer H, Humpfer E, Spraul M, Lewis MR, Pearce JT, Holmes E, Lindon JC and Nicholson JK. Precision high-throughput proton NMR spectroscopy of human urine, serum, and plasma for large-scale metabolic phenotyping. *Anal Chem*. 2014;86:9887-94.

5. Karaman I, Ferreira DL, Boulange CL, Kaluarachchi MR, Herrington D, Dona AC, Castagne R, Moayyeri A, Lehne B, Loh M, de Vries PS, Dehghan A, Franco OH, Hofman A, Evangelou E, Tzoulaki I, Elliott P, Lindon JC and Ebbels TM. Workflow for Integrated Processing of Multicohort Untargeted 1H NMR Metabolomics Data in Large-Scale Metabolic Epidemiology. *J Proteome Res*. 2016;15:4188-4194.

6. Petersen M, Dyrby M, Toubro S, Engelsen SB, Norgaard L, Pedersen HT and Dyerberg J. Quantification of lipoprotein subclasses by proton nuclear magnetic resonance-based partial least-squares regression models. *Clin Chem*. 2005;51:1457-61.

7. Flote VG, Vettukattil R, Bathen TF, Egeland T, McTiernan A, Frydenberg H, Husoy A, Finstad SE, Lomo J, Garred O, Schlichting E, Wist EA and Thune I. Lipoprotein subfractions by nuclear magnetic resonance are associated with tumor characteristics in breast cancer. *Lipids health dis*. 2016;15:56.

8. Navratil V, Pontoizeau C, Billoir E and Blaise BJ. SRV: an open-source toolbox to accelerate the recovery of metabolic biomarkers and correlations from metabolic phenotyping datasets. *Bioinformatics*. 2013;29:1348-9.

9. Blaise BJ, Shintu L, Elena B, Emsley L, Dumas ME and Toulhoat P. Statistical recoupling prior to significance testing in nuclear magnetic resonance based metabonomics. *Anal Chem*. 2009;81:6242-51.

10. Posma JM, Garcia-Perez I, De Iorio M, Lindon JC, Elliott P, Holmes E, Ebbels TM and Nicholson JK. Subset optimization by reference matching (STORM): an optimized statistical approach for recovery of metabolic biomarker structural information from 1H NMR spectra of biofluids. *Anal Chem*. 2012;84:10694-701.

11. Cloarec O, Dumas ME, Craig A, Barton RH, Trygg J, Hudson J, Blancher C, Gauguier D, Lindon JC, Holmes E and Nicholson J. Statistical total correlation spectroscopy: an exploratory approach for latent biomarker identification from metabolic 1H NMR data sets. *Anal Chem*. 2005;77:1282-9.

12. Wishart DS, Jewison T, Guo AC, Wilson M, Knox C, Liu Y, Djoumbou Y, Mandal R, Aziat F, Dong E, Bouatra S, Sinelnikov I, Arndt D, Xia J, Liu P, Yallou F, Bjorndahl T, Perez-Pineiro R, Eisner R, Allen F, Neveu V, Greiner R and Scalbert A. HMDB 3.0--The Human Metabolome Database in 2013. *Nucleic Acids Res*. 2013;41:D801-7.

13. Sumner LW, Amberg A, Barrett D, Beale MH, Beger R, Daykin CA, Fan TW, Fiehn O, Goodacre R, Griffin JL, Hankemeier T, Hardy N, Harnly J, Higashi R, Kopka J, Lane AN, Lindon JC, Marriott P, Nicholls AW, Reily MD, Thaden JJ and Viant MR. Proposed minimum reporting standards for chemical analysis Chemical Analysis Working Group (CAWG) Metabolomics Standards Initiative (MSI). *Metabolomics*. 2007;3:211-221.

14. Willer CJ, Schmidt EM, Sengupta S, Peloso GM, Gustafsson S, Kanoni S, Ganna A, Chen J, Buchkovich ML, Mora S, Beckmann JS, Bragg-Gresham JL, Chang HY, Demirkan A, Den Hertog HM, Do R, Donnelly LA, Ehret GB, Esko T, Feitosa MF, Ferreira T, Fischer K, Fontanillas P, Fraser RM, Freitag DF, Gurdasani D, Heikkila K, Hypponen E, Isaacs A, Jackson AU, Johansson A, Johnson T, Kaakinen M, Kettunen J, Kleber ME, Li X, Luan J, Lyytikainen LP, Magnusson PK, Mangino M, Mihailov E, Montasser ME, Muller-Nurasyid M, Nolte IM, O'Connell JR, Palmer CD, Perola M, Petersen AK, Sanna S, Saxena R, Service SK, Shah S, Shungin D, Sidore C, Song C, Strawbridge RJ, Surakka I, Tanaka T, Teslovich TM, Thorleifsson G, Van den Herik EG, Voight BF, Volcik KA, Waite LL, Wong A, Wu Y, Zhang W, Absher D, Asiki G, Barroso I, Been LF, Bolton JL, Bonnycastle LL, Brambilla P, Burnett MS, Cesana G, Dimitriou M, Doney AS, Doring A, Elliott P, Epstein SE, Eyjolfsson GI, Gigante B, Goodarzi MO, Grallert H, Gravito ML, Groves CJ, Hallmans G, Hartikainen AL, Hayward C, Hernandez D, Hicks AA, Holm H, Hung YJ, Illig T, Jones MR, Kaleebu P, Kastelein JJ, Khaw KT, Kim E, Klopp N, Komulainen P, Kumari M, Langenberg C, Lehtimaki T, Lin SY, Lindstrom J, Loos RJ, Mach F, McArdle WL, Meisinger C, Mitchell BD, Muller G, Nagaraja R, Narisu N, Nieminen TV, Nsubuga RN, Olafsson I, Ong KK, Palotie A, Papamarkou T, Pomilla C, Pouta A, Rader DJ, Reilly MP, Ridker PM, Rivadeneira F, Rudan I, Ruokonen A, Samani N, Scharnagl H, Seeley J, Silander K, Stancakova A, Stirrups K, Swift AJ, Tiret L, Uitterlinden AG, van Pelt LJ, Vedantam

S, Wainwright N, Wijmenga C, Wild SH, Willemsen G, Wilsgaard T, Wilson JF, Young EH, Zhao JH, Adair LS, Arveiler D, Assimes TL, Bandinelli S, Bennett F, Bochud M, Boehm BO, Boomsma DI, Borecki IB, Bornstein SR, Bovet P, Burnier M, Campbell H, Chakravarti A, Chambers JC, Chen YD, Collins FS, Cooper RS, Danesh J, Dedoussis G, de Faire U, Feranil AB, Ferrieres J, Ferrucci L, Freimer NB, Gieger C, Groop LC, Gudnason V, Gyllensten U, Hamsten A, Harris TB, Hingorani A, Hirschhorn JN, Hofman A, Hovingh GK, Hsiung CA, Humphries SE, Hunt SC, Hveem K, Iribarren C, Jarvelin MR, Jula A, Kahonen M, Kaprio J, Kesaniemi A, Kivimaki M, Kooner JS, Koudstaal PJ, Krauss RM, Kuh D, Kuusisto J, Kyvik KO, Laakso M, Lakka TA, Lind L, Lindgren CM, Martin NG, Marz W, McCarthy MI, McKenzie CA, Meneton P, Metspalu A, Moilanen L, Morris AD, Munroe PB, Njolstad I, Pedersen NL, Power C, Pramstaller PP, Price JF, Psaty BM, Quertermous T, Rauramaa R, Saleheen D, Salomaa V, Sanghera DK, Saramies J, Schwarz PE, Sheu WH, Shuldiner AR, Siegbahn A, Spector TD, Stefansson K, Strachan DP, Tayo BO, Tremoli E, Tuomilehto J, Uusitupa M, van Duijn CM, Vollenweider P, Wallentin L, Wareham NJ, Whitfield JB, Wolffenbuttel BH, Ordovas JM, Boerwinkle E, Palmer CN, Thorsteinsdottir U, Chasman DI, Rotter JI, Franks PW, Ripatti S, Cupples LA, Sandhu MS, Rich SS, Boehnke M, Deloukas P, Kathiresan S, Mohlke KL, Ingelsson E and Abecasis GR. Discovery and refinement of loci associated with lipid levels. *Nat Genet*. 2013;45:1274-83.

15. Chu AY, Deng X, Fisher VA, Drong A, Zhang Y, Feitosa MF, Liu CT, Weeks O, Choh AC, Duan Q, Dyer TD, Eicher JD, Guo X, Heard-Costa NL, Kacprowski T, Kent JW, Jr., Lange LA, Liu X, Lohman K, Lu L, Mahajan A, O'Connell JR, Parihar A, Peralta JM, Smith AV, Zhang Y, Homuth G, Kissebah AH, Kullberg J, Laqua R, Launer LJ, Nauck M, Olivier M, Peyser PA, Terry JG, Wojczynski MK, Yao J, Bielak LF, Blangero J, Borecki IB, Bowden DW,

Carr JJ, Czerwinski SA, Ding J, Friedrich N, Gudnason V, Harris TB, Ingelsson E, Johnson AD, Kardia SL, Langefeld CD, Lind L, Liu Y, Mitchell BD, Morris AP, Mosley TH, Jr., Rotter JI, Shuldiner AR, Towne B, Volzke H, Wallaschofski H, Wilson JG, Allison M, Lindgren CM, Goessling W, Cupples LA, Steinhauser ML and Fox CS. Multiethnic genome-wide meta-analysis of ectopic fat depots identifies loci associated with adipocyte development and differentiation. *Nat Genet*. 2017;49:125-130.

16. Taylor AE, Burgess S, Ware JJ, Gage SH, Richards JB, Davey Smith G and Munafo MR. Investigating causality in the association between 25(OH)D and schizophrenia. *Sci Rep*. 2016;6:26496.

17. Leslie R, O'Donnell CJ and Johnson AD. GRASP: analysis of genotype-phenotype results from 1390 genome-wide association studies and corresponding open access database. *Bioinformatics*. 2014;30:i185-94.

18. Burgess S, Davies NM and Thompson SG. Bias due to participant overlap in two-sample Mendelian randomization. *Genet Epidemiol.* 2016;40:597-608.

19. Burgess S, Butterworth A and Thompson SG. Mendelian randomization analysis with multiple genetic variants using summarized data. *Genet Epidemiol*. 2013;37:658-65.

20. Bowden J, Davey Smith G and Burgess S. Mendelian randomization with invalid instruments: effect estimation and bias detection through Egger regression. *Int J Epidemiol.* 2015;44:512-25.

21. Bowden J, Davey Smith G, Haycock PC and Burgess S. Consistent Estimation in Mendelian Randomization with Some Invalid Instruments Using a Weighted Median Estimator. *Genet Epidemiol*. 2016;40:304-14.

22. Hartwig FP, Davey Smith G and Bowden J. Robust inference in summary data Mendelian randomization via the zero modal pleiotropy assumption. *Int J Epidemiol.* 2017;46:1985-1998.

23. R Core Team. R: A Language and Environment for Statistical Computing. R Foundation for Statistical Computing, Vienna, Austria. 2016.

24. Hemani G, Zheng J, Wade KH, Laurin C, Elsworth B, Burgess S, Bowden J, Langdon R, Tan V, Yarmolinsky J, Shihab HA, Timpson N, Evans DM, Relton C, Martin RM, Davey Smith G, Gaunt TR, Haycock PC and The MR-Base Collaboration. MR-Base: a platform for systematic causal inference across the phenome using billions of genetic associations *bioRxiv doi: 101101/078972*. 2016.